Neuropathology 2005; **25**, 381–387

Workshop: Recent Advances in Motor Neuron Disease

Is motoneuronal cell death in amyotrophic lateral sclerosis apoptosis?

Mineo Yamazaki,[1,2] Eisaku Esumi[3] and Imaharu Nakano[4]

[1]Division of Neurology, 2nd Department of Internal Medicine, Nippon Medical School, [2]Department of Neuropathology, Tokyo Metropolitan Institute for Neuroscience, [3]Department of Neurology, Tokyo Tama Hospital, Tokyo and [4]Department of Neurology, Jichi Medical School, Tochigi, Japan

To clarify the controversy concerning whether the cell death of motor neurons in ALS is apoptosis, we investigated the expression of Apaf-1 and caspase-9 mRNA in spinal cord tissue obained at autopsy from patients with ALS and controls using RT-PCR; the presence of *in situ* nuclear DNA fragmentation in motor neurons by the TdT-mediated dUTP-biotin nick end-labeling (TUNEL) method; and immunocytochemical localization of Apaf-1 and caspase-3, which are known as promotors of apoptotic processes. Although Apaf-1 and caspase-9 mRNAs levels were increased in ALS, Apaf-1 immunoreactivity (IR) showed no significant difference between ALS and the control, and caspase-3 IR was not observed in ALS motoneurons, casting doubt on the notion that motor neurons in ALS undergo death by the classic apoptotic pathway. Although TUNEL-positive motor neurons were frequently observed in the anterior horn in ALS, these neurons always showed an atrophic cell body with a shrunken and pyknotic nucleus, indicating that they were at the terminal stage of degeneration. No apoptotic bodies were seen. These findings suggest that the mechanism of motor neuronal cell death in ALS might not be apoptosis, but some other as yet unidentified mechanism.

Key words: amyotrophic lateral sclerosis, Apaf-1, apoptosis, caspase, cell death, DNA fragmentation.

INTRODUCTION

Since the discovery of missense mutations in the chromosome 21 gene which encodes copper/zinc superoxide dismutase-1 (SOD1) in the dominantly inherited ALS family,[1–4] ALS research has focused on this SOD1 gene mutation.[5–9] A number of authors have proposed the possibility of programmed cell death, termed apoptosis, in the motor neurons in SOD1 transgenic mice, and suggested that the same cell death processes also occur in classic ALS in humans.

The definition of apoptosis is so fuzzy, however, as to confound attempts to interpret the results of apoptosis studies over a range of degenerative diseases. This lack of clarity is reflected in inconsistencies in the biochemical and morphological features of motoneuronal cell death observed in SOD1 transgenic mice and in patients with ALS.[10–16]

Several recent investigations of motor neuronal cell death in ALS have focused on caspases and related proteins in SOD1 transgenic mice.[17–20] Caspases are generated in the form of pro-enzymes (inactive form), and are activated by proteolysis to form active complexes which kill neurons via the apoptosis process. The caspases examined in the present study are thought to be associated with mitochondria and to be active in the final common pathway of the caspase cascade. Cytochrome C (Apaf-2) and Apaf-1 are discharged together from mitochondria, and form a complex with caspase-9 through caspase recruitment domain in the presence of dATP. As a result, caspase-9 is changed to the activated form, which in turn activates caspase-3, which finally induces cell death.

To clarify whether apoptosis is in fact associated with the cell death of motoneurons in ALS patients, we studied the presence of DNA fragmentation, the definitive sign of apoptosis, in these cells. In addition, we also analyzed Apaf-1 and caspase-9 mRNA, and immunocytochemically investigated Apaf-1 and caspase-3 in spinal motoneurons in ALS patients.

Correspondence: Mineo Yamazaki, MD, PhD, The 2nd Department of Internal Medicine, Nippon Medical School, 1-1-5 Sendagi, Bunkyo-ku, Tokyo 113-8602, Japan. Email: yamazaki@nms.ac.jp

Received 26 May 2005; accepted 30 May 2005.

MATERIALS AND METHODS

Tissue preparation

The brain and cervical and lumbar segments of the spinal cord were rapidly obtained at autopsy of patients with ALS ($n = 3$), disease controls ($n = 2$, ossification of the posterior longitudinal ligament and MSA) and non-neurological disease controls ($n = 2$, acute myocardial infarction and adrenal gland cancer). All ALS patients showed symptoms of upper and lower motor neuron involvement and fulfilled the pathological criteria of ALS. The tissues obtained at autopsy were preserved, frozen at –80°C until analysis. For the TdT-mediated dUTP-biotin nick end-labeling (TUNEL) method, sections were made from formalin-fixed and paraffin-embedded blocks of the appropriate regions.

RT-PCR method

Total mRNA was isolated from the cerebral cortex (area 17), putamen and spinal cord of ALS patients. Poly A+ mRNA was controlled using a Quickprep mRNA purification kit (Amersham Pharmacia Biotech, Uppsala, Sweden). RT-PCR was performed using the following primers specific to *Apaf-1* and *caspase-9* genes. The sense and antisense primers for *Apaf-1* were 5′-ACATCACGAA TCTTTCCCGC-3′, corresponding to APPN, and 5′-AACACTTCACTATCACTTCC-3′, corresponding to APPC. The primers used for *caspase-9* were 5′-GCCATG GACGAAGCGGATCGGCGG-3′ (sense) and 5′-GGC CTGGATGAAAAAGAGCTGGG-3′ (antisense). PCR was performed with a synthetic first-strand cDNA template. Amplification was continued for 35 cycles (1 min denaturation at 94°C, 1 min annealing at 55°C, 2 min extension at 72°C).

Immunohistochemistry

Immunohistochemical staining was performed using mouse monoclonal anti-Apaf-1 antibody (MAB868; R & D systems, Minneapolis, MN, USA), rabbit polyclonal anti-CPP32 antibody[21] and mouse monoclonal anticaspase-3 antibody (sc-7272; Santa Cruz Biotechnology, CA, USA). Frozen sections were incubated with 3% hydrogen peroxide for 30 min to block endogenous peroxidase activity. The sections were incubated with the antibodies at 4°C overnight and immunoreactivity was visualized with a Histostain SP kit (Zymed, San Francisco, CA, USA).

TUNEL method

Formalin-fixed, paraffin-embedded lumbar cord specimens from six ALS patients were examined in comparison with those from four controls. To facilitate the earliest possible detection of changes in motor neurons, these six cases were selected from among more than 50 ALS cases for their relatively well-preserved anterior horn cells. Mean age of the ALS and control (three with cerebral infarction and one with Marchiafava-Bignami disease) patients was 67 years (range 50–84 years) and 50 years (range 18–70 years), respectively.

DNA fragmentation was detected by the TUNEL method, using an *in situ* cell death detection kit (Boehringer-Mannheim, Indianapolis, MN, USA). Negative controls were examined using TUNEL reaction solution without TdT or fluorescein dUTP. Feasibility of the nuclear labeling of cells by the TUNEL method was confirmed in intestinal tissue obtained at autopsy of patients with malignant lymphoma. After oligonucleosomal DNA cleavages were labeled, photos of each TUNEL-positive neuron were taken, the same specimens were stained with HE, and TUNEL-positive neurons identified from the

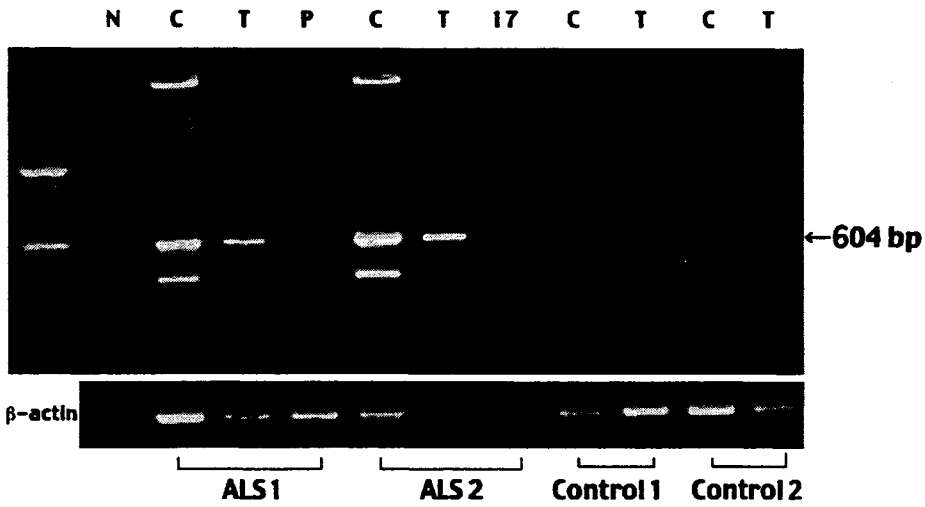

Fig. 1 Detection of Apaf-1 mRNA in the brains of control and ALS patients. β-actin mRNA in the same samples was used as control. The Apaf-1 mRNA band was detected in the cervical and thoracic cord, and was compared with cerebral cortex and putamen in patients with ALS (N: negative control, C: C8, T: Th12, P: putamen, 17: area 17).

photos were cytopathologically observed. TUNEL-positive spinal motor neurons and all anterior motor neurons in all sections were counted, and the frequency of TUNEL-positive spinal motor neurons was measured.

RESULTS

PT-PCR

PCR using primers to amplify *Apaf-1* clearly revealed positive bands of Apaf-1 mRNA in the cervical (C8) and thoracic cord (T12) in patients with ALS, but not in the cerebral cortex and putamen as such. In contrast, Apaf-1 mRNA was scarcely detected in the spinal cord of control cases (Fig. 1). Apaf-1 mRNA was clearly expressed in the putamen and cervical cord of patients with MSA (Fig. 2). The caspase-9 mRNA band was detected in the spinal cord of ALS patients and putamen and cervical cord of MSA patients, but was hardly seen in control cases (Fig. 3).

Immunocytochemistry

To determine whether Apaf-1 and caspase-3 are activated in ALS, control and ALS brains were immunostained with anti-Apaf-1 and anticaspase-3 antibodies. For Apaf-1, anterior horn motoneurons in control and ALS spinal cords showed weak cytoplasmic staining for Apaf-1, whereas ALS brains showed no significant differences to control brains (Fig. 4a,b). Immunolabeling using antibodies specific to caspase-3, rabbit polyclonal anti-CPP32 antibody (Fig. 4c,d) and mouse monoclonal anticaspase-3 antibody (Fig. 4e,f) revealed only scarce caspase-3 immunoreactivity in motor neurons in control and ALS brains.

TUNEL method

TUNEL-positive motor neurons in the anterior horn were observed in three of six ALS cases, whereas in control cases only two TUNEL-positive neurons were seen, one each in two cases. The TUNEL-positive motor neurons were atrophic and round in both groups, without large cell processes. They were filled with lipofuscin and the nucleus was eccentric, flat and pyknotic (Fig. 5a,b). Although TUNEL-positive motor neurons with Lewy body-like hyaline inclusions were occasionally found (Fig. 5c,d), no TUNEL-positive neurons carrying Bunina bodies were observed.

Not all atrophic anterior horn neurons were TUNEL-positive; some had TUNEL-negative nuclei, which were always a generally round shape with a light nucleoplasm. (Fig. 5e,f). However, most TUNEL-negative neurons were of normal size and had many processes in their cell bodies. TUNEL-positive motor neurons represented 5.3–8.9% of

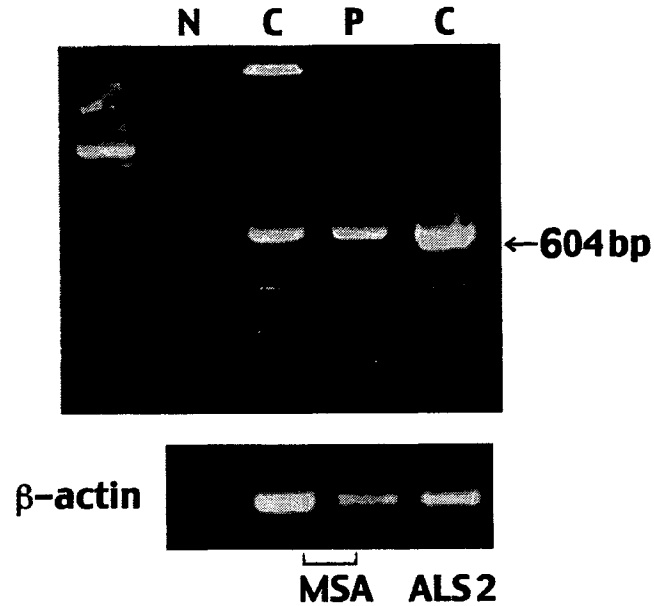

Fig. 2 Detection of Apaf-1 mRNA in the brains of MSA patients. Apaf-1 mRNA was expressed in the putamen and cervical cord of a patient with MSA (N: negative control, C: C8, P: putamen).

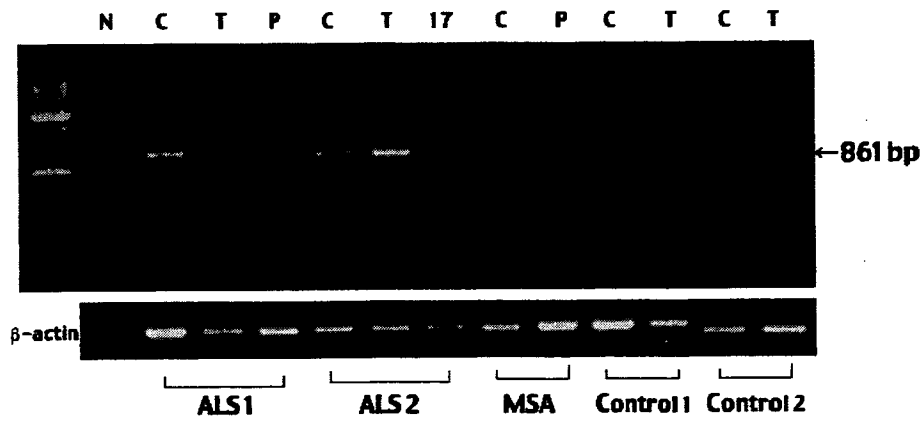

Fig. 3 Expression of caspase-9 mRNA in control, MSA and ALS brains. The caspase-9 mRNA band was detected in the spinal cord of ALS patients and in the putamen and cervical cord of MSA patients, but not in control case tissues (N: negative control, C: C8, T: Th12, P: putamen, 17: area 17).

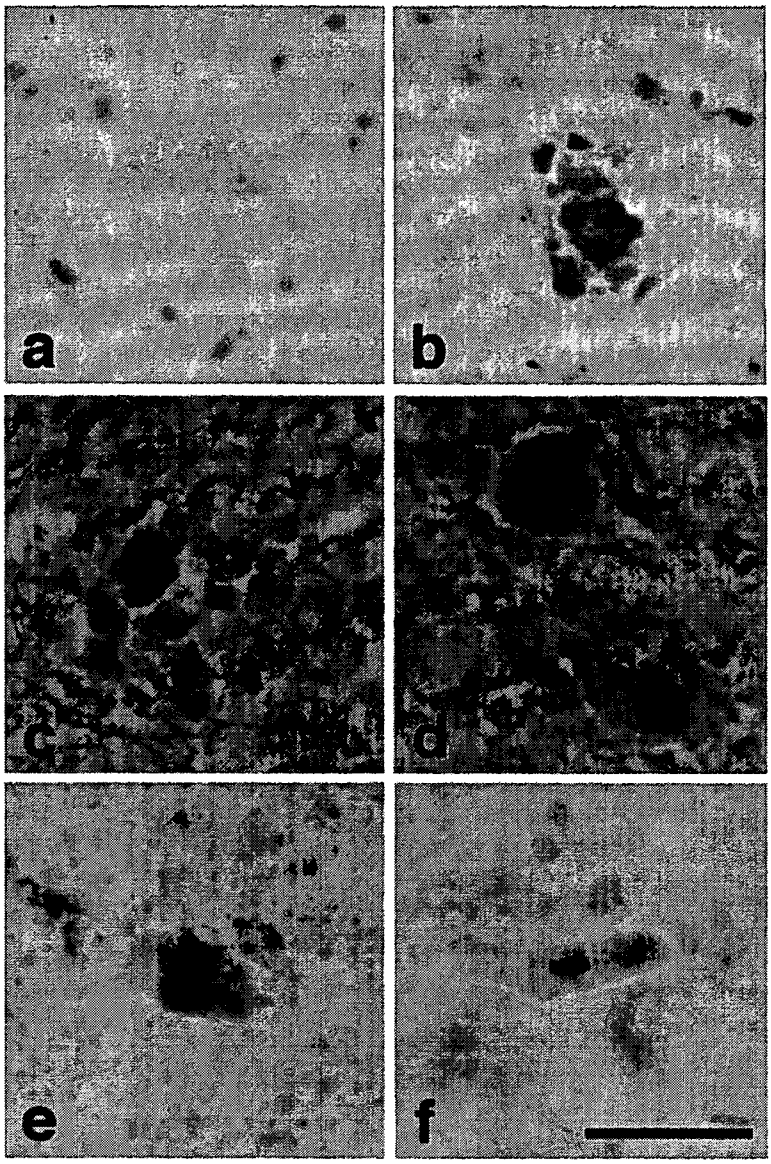

Fig. 4 Immunohistochemical expression of Apaf-1 and caspase-3 in the spinal cord of control and ALS patients. (a,b) No difference in Apaf-1 immunostaining between ALS (a) and control (b) cervical cords (C8). (c,d) Immunolabeling using rabbit polyclonal anti-CPP32 antibody showed no immunoreactivity in anterior horn neurons of control (c) or ALS (d) lumbar cords (L5). (e,f) Mouse monoclonal anticaspase-3 antibody revealed almost no immunoreactivity of caspase-3 in motor neurons in ossification of the posterior longitudinal ligament (e) or ALS (f) cervical cords (C8). Bar, 100 μm.

all anterior horn neurons (Table 1), and all motor neurons with a normal appearance were TUNEL-negative. No apoptotic bodies were seen in any ALS patient specimen.

DISCUSSION

For several reasons, the findings of this study on whether neurons in ALS undergo apoptosis were inconclusive. Although mRNAs of Apaf-1 and caspase-9 were apparently expressed in ALS brains, indicating that apoptosis through *Apaf-1* and *caspase-9* may be, at least to some extent, involved in this neuronal cell death, expression was not restricted to the ALS brain but was also recognized to some degree in the MSA brain. Further, we could not determine whether Apaf-1 mRNA and caspase-9 mRNA in the ALS brains were expressed by neurons, glia, or both. Indeed, our immunocytochemical investigation of Apaf-1, caspase-9 and caspase-3 failed to show any substantial increase in the production of these proteins in ALS over control brains. Against these findings, however, it was recently reported that caspase-9 is activated in spinal motor neurons of ALS patients.[22] It thus remains unclear whether caspase-9 is activated in motor neurons of ALS brains. In our study, caspase-9 mRNA was expressed in ALS brains and was clearly activated in motor neurons of the ALS spinal cord. However, our data also suggest that caspase-3 was not activated in the spinal motor neuron, and it was unlikely that the apoptotic cascade from caspase-9 to caspase-3 was present.

The phenomenon apoptosis was originally defined as fulfilling the following conditions: (i) DNA fragmentation;

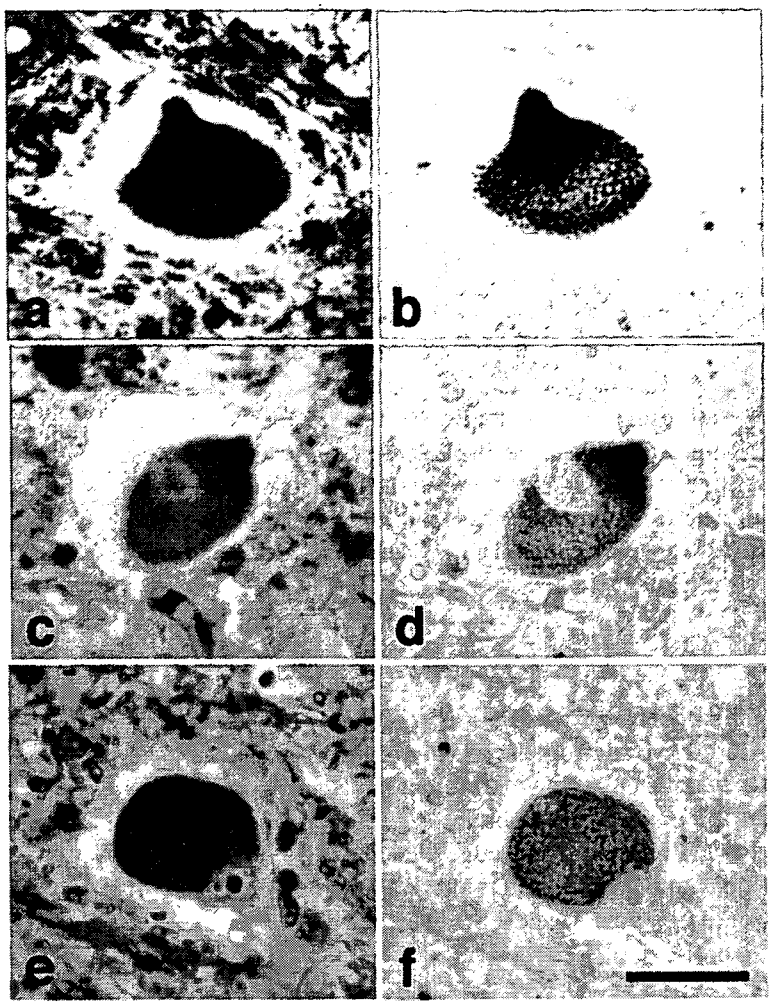

Fig. 5 TdT-mediated dUTP-biotin nick end-labeling (TUNEL) staining of anterior horn neurons in ALS patients. (a,b) A TUNEL-positive lumbar motor neuron is seen (case 1). The cell body is round and filled with lipofuscin. The same section stained with HE stain (a) and the TUNEL method (b). (c,d) TUNEL staining was occasionally observed in motor neurons with hyaline inclusions. (e,f) Some TUNEL-negative anterior horn neurons were atrophic and filled with lipofuscin. Bar, 50 μm.

Table 1 Positive TdT-mediated dUTP-biotin nick end-labeling (TUNEL) of ALS spinal motor neurons

Case	Age (years), sex	Total no. neurons (no.sections)	TUNEL-positive neurons	Mean % positive per section
1	61, female	486 (10)	26	5.3
2	81, female	219 (5)	13	5.9
3	67, male	202 (10)	18	8.9

and (ii) nuclear fragmentation and cellular budding (the presence of apoptotic bodies). Given the inconclusive PCR and immunocytology results here, we also checked whether the morphological changes of motor neurons in ALS were compatible with this definition. Results using the TUNEL method showed the presence of *in situ* DNA fragmentation in 5–9% of spinal motor neurons in ALS patients. If this DNA fragmentation does in fact represent a process of apoptosis, and if apoptotic cell death in motoneurons proceeds over a few hours as seen in other organs, this high proportion of TUNEL-positive cells would result in the total mathematical disappearance of spinal motor neurons in only a few months, with patients of course dying long before. In reality, however, the typical clinical course of several years before death means that one or both of the above assumptions is wrong. Although the possibility that apoptosis occurs more slowly in *in situ* motor neurons than other organ cells cannot be denied, *in vitro* studies using neuronal cell cultures[23] and our present finding that all TUNEL-positive neurons had shrunken pyknotic nuclei suggest that the mechanism of motor neuronal cell death in ALS represents a different process to apoptosis as defined above.

Moreover, it has been reported that the formation of apoptotic bodies was completed within several minutes in cells of a culture system.[24] Further, *in vivo*, apoptotic bodies disappear within only a few hours after formation in organs such as the liver.[25] If this is the case for motoneu-

rons also, this rapid time course may explain why apoptotic bodies can hardly be detected in human brain tissue. DNA fragmentation detected by the TUNEL method, however, is considered to represent an early stage of apoptosis, so specimens containing frequent TUNEL-positive neurons undergoing apoptosis should show at least some apoptotic bodies. This was not the case for our ALS specimens, implying again that the DNA fragmentation we observed may not be related to apoptosis. The present study thus fails to corroborate several reports indicating the apoptotic processes of motoneuronal cell death in ALS.[26–28] ALS is a lethal disease without effective therapy, so the exploration of new drugs and therapies on the basis of immature hypotheses of pathomechanisms is both valid and necessary. At the same time, however, it is necessary to pursue investigations into the cause and mechanism of this difficult disease via a rational and critical observation and analysis of patient tissues.

ACKNOWLEDGMENTS

The authors wish to express their gratitude to Dr Nobutaka Arai, Tokyo Metropolitan Institute for Neuroscience, and Dr Masaya Oda, Tokyo Metropolitan Neurological Hospital, for the donation of brain tissues used in this study. We also gratefully acknowledge the helpful support of Dr Kunihiko Ikeguchi and Dr Mitsuya Morita, Department of Neurology, Jichi Medical School.

REFERENCES

1. Deng HX, Hentati A, Tainer JA *et al.* Amyotrophic lateral sclerosis and structural defects in Cu, Zn superoxide dismutase. *Science* 1993; **261**: 1047–1051.
2. Aoki M, Ogasawara M, Matsubara Y *et al.* Mild ALS in Japan associated with novel SOD mutation. *Nat Genet* 1993; **5**: 323–324.
3. Elshafey A, Lanyon WG, Connor JM. Identification of a new missense point mutation in exon 4 of the Cu/Zn superoxide dismutase (SOD-1) gene in a family with amyotrophic lateral sclerosis. *Hum Mol Genet* 1994; **3**: 363–364.
4. Nakano R, Sato S, Inuzuka T *et al.* A novel mutation in Cu/Zn superoxide dismutase gene in Japanese familial amyotrophic lateral sclerosis. *Biochem Biophys Res Commun* 1994; **200**: 695–703.
5. Gurney ME, Pu H, Chiu AY *et al.* Motor neuron degeneration in mice that express a human Cu, Zn superoxide dismutase mutation. *Science* 1994; **264**: 1772–1775.
6. Tsuda T, Munthasser S, Fraser PE *et al.* Analysis of the functional effects of a mutation in SOD1 associated with familial amyotrophic lateral sclerosis. *Neuron* 1994; **13**: 727–736.
7. Dal Canto MC, Gurney ME. Development of central nervous system pathology in a murine transgenic model of human amyotrophic lateral sclerosis. *Am J Pathol* 1994; **145**: 1271–1279.
8. Durham HD, Roy J. Dong L, Figlewicz DA. Aggregation of mutant Cu/Zn superoxide dismutase proteins in a culture model of ALS. *J Neuropathol Exp Neurol* 1997; **56**: 523–530.
9. Ghadge GD, Lee JP, Bindokas VP *et al.* Mutant superoxide dismutase-1-linked familial amyotrophic lateral sclerosis: molecular mechanisms of neuronal death and protection. *J Neurosci* 1997; **17**: 8756–8766.
10. Migheli A, Cavalla P, Marino S, Schiffer D. A study of apoptosis in normal and pathologic nervous tissue after in situ end-labeling of DNA strand breaks. *J Neuropathol Exp Neurol* 1994; **53**: 606–616.
11. Rabizadeh S, Gralla EB, Borchelt DR *et al.* Mutations associated with amyotrophic lateral sclerosis convert superoxide dismutase from an antiapoptotic gene to a proapoptotic gene: studies in yeast and neural cells. *Proc Natl Acad Sci USA* 1995; **92**: 3024–3028.
12. Troost D, Aten J, Morsink F, de Jong JMBV. Apoptosis in amyotrophic lateral sclerosis is not restricted to motor neurons. Bcl-2 expression is increased in unaffected post-central gyrus. *Neuropathol Appl Neurobiol* 1995; **21**: 498–504.
13. Troy CM, Shelanski ML. Down-regulation of coper/zinc superoxide dismutase causes apoptotic death in PC12 neuronal cells. *Proc Natl Acad Sci USA* 1994; **91**: 6384–6387.
14. Yoshiyama Y, Yamada T, Asanuma K, Asahi T. Apoptotic related antigen, LeY and nick-end labeling are positive in spinal motor neurons in amyotrophic lateral sclerosis. *Acta Neuropathol* 1994; **88**: 207–211.
15. Mu X, He J, Anderson DW, Trojanowski JQ, Springer JE. Altered expression of bcl-2 and bax mRNA in amyotrophic lateral sclerosis spinal cord motor neurons. *Ann Neurol* 1996; **40**: 379–386.
16. Martin LJ. Neuronal death in amyotrophic lateral sclerosis is apoptosis: possible contribution of a programmed cell death mechanism. *J Neuropathol Exp Neurol* 1999; **58**: 459–471.
17. Pasinelli P, Borchelt DR, Houseweart MK, Cleveland DW, Brown RH Jr. Caspase-1 is activated in neural cells and tissue with amyotrophic lateral sclerosis-associated mutations in copper-zinc superoxide dismutase. *Proc Natl Acad Sci USA* 1998; **95**: 15763–15768.
18. Li M, Ona VO, Guegan C *et al.* Functional role of caspase-1 and caspase-3 in an ALS transgenic mouse model. *Science* 2000; **288**: 335–339.

19. Takeuchi H, Kobayashi Y, Ishigaki S, Doyu M, Sobue G. Mitochondrial localization of mutant superoxide dismutase 1 triggers caspase-dependent cell death in a cellular model of familial amyotrophic lateral sclerosis. *J Biol Chem* 2002; **277**: 50966–50972.
20. Kang SJ, Sanchez I, Jing N, Yuan J. Dissociation between neurodegeneration and caspase-11-mediated activation of caspase-1 and caspase-3 in a mouse model of amyotrophic lateral sclerosis. *J Neurosci* 2003; **23**: 5455–5460.
21. Krajewska M, Wang HG, Krajewski S *et al.* Immunohistochemical analysis of in vivo patterns of expression of CPP32 (Caspase-3), a cell death protease. *Cancer Res* 1997; **57**: 1605–1613.
22. Inoue H, Tsukita K, Iwasato T *et al.* The crucial role of caspase-9 in the disease progression of a transgenic ALS mouse model. *EMBO J* 2003; **22**: 6665–6674.
23. Kaasik A, Vassiljev V, Poldoja E, Kalda A, Zharkovsky A. Do nuclear condensation or fragmentation and DNA fragmentation reflect the mode of neuronal death? *Neuroreport* 1999; **10**: 1937–1942.
24. Matter A. Microcinematographic and electron microscopic analysis of target cell lysis induced by cytotoxic T lymphocytes. *Immunology* 1979; **36**: 179–190.
25. Bursch W, Paffe S, Putz B, Barthel G, Schulte-Hermann R. Determination of the length of the histological stages of apoptosis in normal liver and in altered hepatic foci of rats. *Carcinogenesis* 1990; **11**: 847–853.
26. Kihira T, Yoshida S, Hironishi M, Wakayama I, Yase Y. Neuronal degeneration in amyotrophic lateral sclerosis is mediated by a possible mechanism different from classical apoptosis. *Neuropathology* 1998; **18**: 301–308.
27. Migheli A, Aztori C, Piva R *et al.* Lack of apoptosis in mice with ALS. *Nature Med* 1999; **5**: 966–967.
28. He BP, Strong MJ. Motor neuronal death in sporadic amyotrophic lateral sclerosis (ALS) is not apoptotic. A comparative study of ALS and chronic aluminum chloride neurotoxicity in New Zealand white rabbits. *Neuropathol Appl Neurobiol* 2000; **26**: 150–160.

Available online at www.sciencedirect.com
ScienceDirect
Experimental Neurology 207 (2007) 195–202
Experimental Neurology
www.elsevier.com/locate/yexnr

Hepatocyte growth factor promotes the number of PSD-95 clusters in young hippocampal neurons

Midori Nakano [a], Norio Takagi [a,*], Keiko Takagi [a], Hiroshi Funakoshi [b], Kunio Matsumoto [b,1], Toshikazu Nakamura [b], Satoshi Takeo [a]

[a] *Department of Molecular and Cellular Pharmacology, Tokyo University of Pharmacy and Life Sciences, 1432-1 Horinouchi, Hachioji, Tokyo 192-0392, Japan*
[b] *Division of Molecular Regenerative Medicine, Department of Biochemistry and Molecular Biology, Osaka University Graduate School of Medicine, 2-2-B7 Yamadaoka, Suita, Osaka 565-0871, Japan*

Received 21 April 2007; revised 30 May 2007; accepted 15 June 2007
Available online 26 June 2007

Abstract

Hepatocyte growth factor (HGF) and its receptor are expressed in various regions of the brain and have protective effects against excitotoxic injuries. However, their effects on synapse formation remain to be elucidated. To determine whether HGF has the ability to alter synaptic function during development, we investigated changes in the number of synapse detected by double immunostaining for NMDA receptor subunits and a presynaptic marker in cultured young hippocampal neurons. Whereas application of HGF increased the number of cluster of synapsin, a presynaptic protein, the clusters of NMDA receptor subunits NR1 and NR2B were not altered. Interestingly, colocalization of PSD-95, a scaffolding protein of the receptor, with synapsin was increased by HGF treatment without a change in the total amount of it. In addition, we investigated the expression of surface NMDA receptor, neuroligin, and neurexin, which were assessed by use of a cell-surface biotinylation assay. The application of HGF did not change the surface expression of these proteins. Furthermore, we determined the release of glutamate in response to depolarization. Treatment with HGF promoted depolarization-evoked release of glutamate. These results suggest that HGF modulates the expression of the scaffolding protein of the NMDA receptor at the synapse and promotes maturation of excitatory synapses in young hippocampal neurons.

Keywords: Hepatocyte growth factor; *N*-methyl-D-aspartate receptor; PSD-95

Introduction

The postsynaptic density (PSD), which underlies the postsynaptic membrane at excitatory synapses, links receptors of the neurotransmitter to intracellular signaling proteins and to the cytoskeleton (Kennedy, 1997; Kim and Sheng, 2004; Klauck and Scott, 1995; Ziff, 1997). The *N*-methyl-D-aspartate (NMDA) receptor, a glutamate-gated ion channel, is localized to the PSD at excitatory synapses in the brain and plays a pivotal role in the regulation of neuronal development and learning function. NMDA receptors are heteromeric complexes of NR1 and NR2A-NR2D or NR3 subunits (Das et al., 1998; Ishii et al., 1993; Monyer et al., 1992; Moriyoshi et al., 1991; Nakanishi, 1992; Nishi et al., 2001). Whereas NR1 is the principal subunit for the activity of the NMDA receptor, the NR2 subunits serve to modulate channel properties of these receptors (Hollmann and Heinemann, 1994). PSD-95, a major protein component of the PSD, interacts with NR2A and NR2B subunits and is thought to regulate channel activities, insertion, and internalization of the NMDA receptor (Lavezzari et al., 2004; Lin et al., 2004; Roche et al., 2001). As synaptic targeting and regulation of activities of NMDA receptors play an important role in synaptic plasticity, PSD-95 could be involved in the regulation of synaptic transmission. In this sense, neuroligin, a binding partner of PSD-95, connects the PSD to presynaptic terminals by binding between the extracellular domain of neuroligin and that of neurexin, a presynaptic binding partner (Dean and Dresbach, 2006). These findings suggest that pre- and

* Corresponding author.
E-mail address: takagino@ps.toyaku.ac.jp (N. Takagi).
[1] Present address: Division of Tumor Dynamics and Regulation, Cancer Research Institute, Kanazawa University, Kanazawa, Japan.

0014-4886/$ - see front matter © 2007 Elsevier Inc. All rights reserved.
doi:10.1016/j.expneurol.2007.06.007

postsynaptic protein complexes modulate structural and functional coordination at synapses in the brain. Neurotrophic factors are known to play an important role in the development of the central nervous system.

Hepatocyte growth factor (HGF), which was originally identified and cloned as a mitogen for hepatocytes (Nakamura et al., 1984, 1989), elicits diverse cellular responses such as mitogenic, motogenic, and morphogenic activities in various types of cells (Matsumoto and Nakamura, 1996; Zarnegar and Michalopoulos, 1995). Although HGF has physiological roles as acting as an organotropic for regeneration and protection of a variety of organs (Balkovetz and Lipschutz, 1999; Matsumoto and Nakamura, 1996, 2001; Zarnegar and Michalopoulos, 1995), exogenous HGF attenuates ischemia-induced injuries under pathophysiological conditions, including cardiac ischemia and reperfusion (Nakamura et al., 2000) and hind limb ischemia (Morishita et al., 1999; Van Belle et al., 1998). HGF and its receptor c-Met were found to be expressed in various regions of the brain and to function in a variety of ways in the central nervous system (Achim et al., 1997; Honda et al., 1995; Sun et al., 2002a,b). Therefore, HGF might have the ability to prevent brain injuries under pathophysiological conditions. Indeed, we previously demonstrated that administration of HGF prevented ischemic brain injuries and also improved learning and memory dysfunction of ischemic rats (Date et al., 2004; Niimura et al., 2006). Although overactivation of the NMDA receptor is associated with degenerative diseases (Dingledine et al., 1999), this receptor plays a key role in the regulation of neuronal development and learning function. Whereas HGF is likely to play an important role during brain development (Giacobini et al., 2007; Ohya et al., 2007), it is still not fully clarified whether HGF affects the development of excitatory synapses, including those bearing NMDA receptors. To determine the role of HGF in the regulation of synaptogenesis, we investigated the effect of HGF on synaptic clustering of NMDA receptor subunits and PSD-95 in cultured hippocampal young neurons. The results obtained show that HGF increased the number of PSD-95 clusters without changing the number of clusters and surface expression of NMDA receptor subunits. Furthermore, HGF promoted depolarization-evoked glutamate release.

Methods

Recombinant HGF

Human recombinant HGF was purified from conditioned medium of Chinese hamster ovary cells transfected with an expression vector containing human HGF cDNA as described earlier (Nakamura et al., 1989). The purity of the human recombinant HGF was >98%, as determined by SDS–PAGE.

Primary hippocampal cultures

Primary hippocampal cell cultures were prepared from fetal rats at gestational day 18 as described previously (Huettner and Baughman, 1986), with slight modifications (Ishihara et al., 2005). The pooled hippocampi were dissociated by incubation at 37 °C for 30 min in Hank's balanced salt solution containing 15 U/mL papain, 210 U/mL deoxyribonuclease I, 1 mM L-cysteine, and 0.5 mM EDTA. The dispersed cells were resuspended in Dulbecco's Modified Eagle's Medium containing 10% horse serum and were plated at a density of 40,000 cells/cm^2 in 35-mm dishes coated with poly-L-lysine. At 24 h after plating, the medium was replaced with serum-free neurobasal medium containing 2% B27 supplements (Gibco-BRL, Rockville, MD, USA) and 0.5 mM glutamine. To inhibit proliferation of non-neuronal cells, we added cytosine arabinoside (1 μM) to each dish. At 3 days *in vitro* (DIV), one-half of the medium was replaced with fresh Neurobasal medium having the 2% B27 supplements and 0.5 mM glutamine. Cultures were maintained at 37 °C in a 5% CO_2 incubator. HGF (30 ng/mL) was added to cultured hippocampal cells at 4 DIV, and then the cultures were maintained for the next 3 days. The dose of used in the present study, 30 ng/mL, was based on the data of Korhonen et al. (2000), Ueda et al. (2001), and those obtained in our preliminary study: treatment with 10 ng/mL HGF increased tyrosine phosphorylation of c-Met protein at 4 DIV to a lesser degree than that with 30 ng/mL HGF.

For experiment on high K^+-evoked glutamate release, hippocampal cells were depolarized for 1 min at 37 °C with 10 mM HEPES buffer, pH 7.4, containing 60 mM KCl, 67 mM NaCl, 2 mM $CaCl_2$–$2H_2O$, 10 mM D-glucose. The collected samples were derivatized with *o*-phthalaldehyde and then injected into a high-performance liquid chromatograph (EICOM, Kyoto, Japan).

Immunohistochemistry

After cells had been fixed in −20 °C methanol, they were then incubated for 1 h at 37 °C or overnight at 4 °C with a primary antibody, and then with the secondary antibody for 1 h. They were then incubated with another primary antibody for 1 h at 37 °C and subsequently with the corresponding secondary antibody for 1 h at 37 °C. The primary antibodies used were mouse anti-NR1 (BD Biosciences), mouse anti-NR2B (BD Biosciences), mouse anti-PSD-95 (Affinity BioReagents), and rabbit anti-synapsin (Affinity BioReagents) antibodies. The secondary antibody used for anti-NR1, anti-NR2B, and anti-PSD-95 antibodies was Cy3-conjugated anti-mouse IgG (Amersham) antibody; and that for anti-synapsin was biotinylated anti-rabbit IgG (Vector Laboratories), which was visualized with Streptavidin FITC (Amersham). Images of cells were captured by a CCD camera (DP50) mounted on an Olympus BX52 microscope equipped with a mercury arc lamp. Images were processed by using Adobe Photoshop (Adobe Systems, Mountain View, CA). To count the number of clusters, we evaluated at least 1 dendrite (50-μm length) in each of 5 randomly selected cells in each of 5 separate cultures. The number of NR1-, NR2B-, PSD-95-, or synapsin I-positive clusters and synapsin I-positive clusters, which were colocalized with NR1, NR2B, or PSD-95, on basal dendritic segments were counted manually. The microscopic observations were performed by a person unaware of the study group.

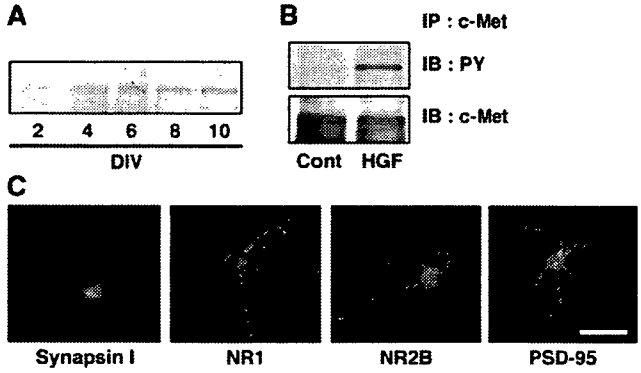

Fig. 1. (A) Proteins from hippocampal cells cultured for 2, 4, 6, 8 or 10 days *in vitro* were analyzed by immunoblotting with anti-c-Met antibody. (B) Proteins from cultured hippocampal cells at 0 (Cont) and 10 min after treatment with 30 ng/mL HGF were immunoprecipitated (IP) with anti-c-Met antibody, and the precipitates were then analyzed by immunoblotting (IB) with anti-phosphotyrosine antibody (PY). The blots were stripped and then re-probed with antibody against c-Met. (C) Cultured hippocampal cells were fixed at 4 days *in vitro* and immunostained with anti-synapsin I, anti-NR1, anti-NR2B, or anti-PSD-95 antibodies. Scale bar represents 25 μm.

Cell-surface biotinylation assay

Cell-surface biotinylation assay of hippocampal neurons was performed as described previously (Shen et al., 2000) with minor modifications. Cultured hippocampal neurons were washed 3 times with ice-cold PBS, pH 7.4, containing 10 mM Na_2HPO_4, 2.7 mM KCl, 137 mM NaCl, 1.0 mM $CaCl_2$, and 0.5 mM $MgCl_2$. Surface proteins were then biotinylated with 1.0 mg/ml sulfo-NHS-SS-biotin (Pierce, Rockford, IL) for 20 min in PBS at 4 °C. To remove unreacted sulfo-NHS-SS-biotin, we washed the cells 3 times with ice-cold 50 mM Tris/PBS, pH 7.4, containing 10 mM Na_2HPO_4, 2.7 mM KCl, 137 mM NaCl, 1.0 mM $CaCl_2$, and 0.5 mM $MgCl_2$. The cells were then lysed with ice-cold lysis buffer (10 mM sodium phosphate, pH 7.4, containing 100 mM NaCl, 0.2% SDS, 5 mM EDTA, 5 mM EGTA, 1 mM sodium orthovanadate, 10 mM sodium pyrophosphate, 10 μM PMSF, 5 μg/ml each of antipain, aprotinin, and leupeptin). For isolation of biotinylated proteins, we used UltraLink-immobilized neutravidin beads (Pierce). After incubation, the beads were washed and bound proteins were eluted with SDS sample buffer.

Western immunoblotting

Hippocampal cells were homogenized in ice-cold 0.32 M sucrose containing 0.2 mM sodium orthovanadate, 0.1 mM phenylmethylsulfonyl fluoride, and 5 μg/ml each of antipain, aprotinin, and leupeptin. Samples were stored at −80 °C until used and were thawed only once. Proteins were solubilized by heating at 100 °C for 5 min in SDS sample buffer (10% glycerol, 5% β-mercaptoethanol, and 2% SDS in 62.5 mM Tris–HCl, pH 6.8) and were separated on polyacrylamide gels. Protein blots were reacted with the appropriate antibodies, and the bound antibody was detected by the enhanced chemiluminescence method (Amersham Biosciences Inc., Piscataway, NJ, USA). Quantification of the immunoreactive bands was performed by using an image analyzer (ATTO Co., Tokyo, Japan). Care was taken to ensure that bands to be semiquantified were in the linear range of response.

Antibodies used for immunoblotting were anti-c-Met (Santa Cruz Biotechnology, Inc., Santa Cruz, CA, USA), anti-phosphotyrosine (clone 4G10, Upstate Biotechnology, Inc., Lake Placid, NY, USA), anti-NR1 (BD Biosciences, San Jose, CA), anti-NR2B (BD Biosciences), anti-PSD-95 (Affinity BioReagents), anti-GluR1 (Upstate Biotechnology), anti-synapsin (Affinity BioReagents), anti-neuroligin 1 (Synaptic Systems, Göttingen, Germany), and rabbit anti-neurexin (Calbiochem) antibodies.

Statistics

The results were expressed as the means±SEM. Statistical comparison between 2 groups was evaluated by using Student's *t*-test. Differences with a probability of 5% or less were considered to be significant ($p<0.05$).

Results

First, we examined the protein expression of HGF receptor c-Met in cultured hippocampal cells at 2, 4, 6, 8, and 10 DIV. In agreement with the results of previous studies (Hossain et al., 2002; Machide et al., 1998), c-Met protein (140 kDa) was expressed in the cultured hippocampal cells throughout the culture period (Fig. 1A). To determine whether c-Met proteins in the young hippocampal cells could be activated in response to the application of HGF, we examined the tyrosine phosphorylation of c-Met after HGF treatment. The tyrosine phosphorylation of c-Met was elevated relative to the initial amount at 10 min after the application of HGF without any change in the amount of total c-Met protein (Fig. 1B). By immunohistochemical analysis, we detected the expression of NMDA receptor subunits NR1 and NR2B, PSD-95, and the presynaptic marker synapsin I at 4 DIV (Fig. 1C). Attempts to examine clustering of NR2A subunits by using several different commercially available NR2A specific antibodies were not successful.

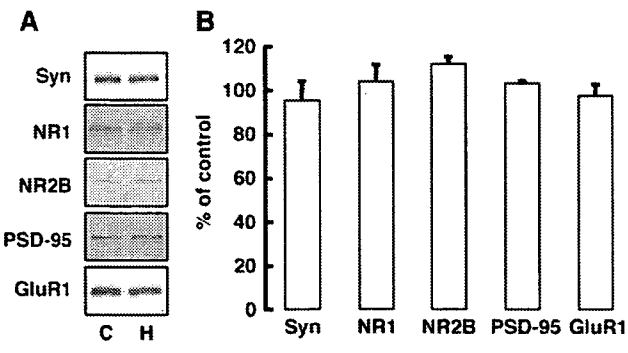

Fig. 2. (A) After 4 days in culture, hippocampal cells were incubated for 3 days with (H) or without (C) 30 ng/mL HGF. Total proteins were analyzed by immunoblotting with anti-synapsin I (Syn), anti-NR1, anti-NR2B, anti-PSD-95, or anti-GluR1 antibodies. (B) Bands corresponding to synapsin I, NR1, NR2B, PSD-95, and GluR1 on immunoblots were scanned. Comparison between HGF-treated (H) and -untreated (C) groups was done using scanned optical densities ($n=4$ each). Results are expressed as the average percentages of the HGF-untreated group±SEM of 4 separate cultures.

Next, we determined the effects of HGF on total amounts of synapsin I, NMDA receptor subunits, and PSD-95 at 7 DIV. As shown Fig. 2, total amounts of these proteins after the application of HGF were comparable to those under normal conditions. Total amount of GluR1 subunit of the α-amino-3-hydroxy-5-methyl-4-isoxazole propionic acid (AMPA) was also comparable to that under normal condition (Fig. 2).

Then, we examined the effects of HGF on clustering and synaptic localization of the NMDA receptor subunits and PSD-95 at 7 DIV. Whereas the number of clusters of presynaptic marker synapsin I was increased at 7 DIV ($F=1.017$, $p=0.036$, Fig. 3; $F=0.227$, $p=0.047$, Fig. 4; $F=0.893$, $p<0.0001$, Fig. 5), there was no change in the number of NR1 (Fig. 3) or NR2B (Fig. 4) subunit clusters. The number of double-positive immunofluorescent puncta containing NR1 (Fig. 3) or NR2B (Fig. 4) subunit and synapsin I after HGF treatment was comparable to that under normal conditions. In contrast, HGF increased the number of PSD-95 clusters ($F=0.617$, $p=0.002$, Fig. 5) and that of PSD-95 clusters colocalized with synapsin I (merge) at 7 DIV ($F=0.915$, $p<0.0001$, Fig. 5). We also examined the effect of HGF on clustering of GluR1 subunit of the AMPA receptor. GluR1 staining showed the diffuse pattern during the first week in culture. The finding was consistent with previous results (Rao et al., 1998). We could not show the data for GluR1 in the present study, as it was difficult to demonstrate the effect of HGF on distinct GluR1 clusters along the dendrites.

Furthermore, to examine the surface expression of the NMDA receptor, we performed a cell-surface biotinylation assay at 7 DIV. Treatment with HGF did not affect the surface expression of

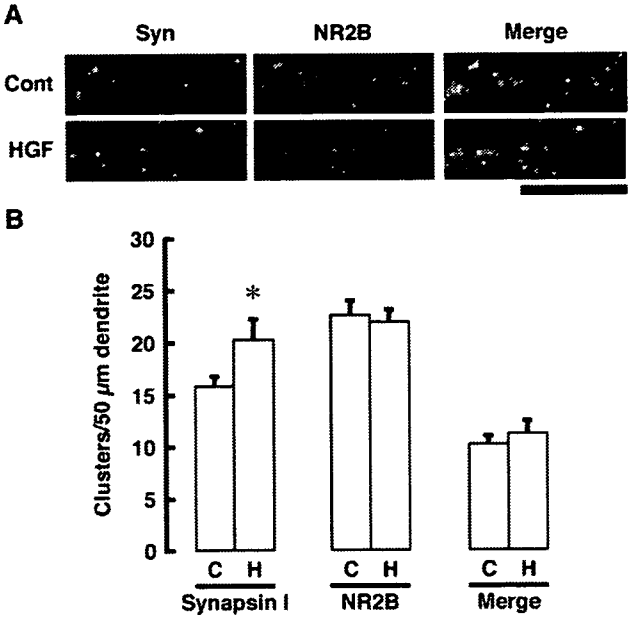

Fig. 4. (A) Hippocampal cells were cultured for 4 days and then treated (H) or not (C) with 30 ng/mL HGF for the following 3 days. The cells were fixed and double-immunostained with anti-synapsin I (for Syn) and anti-NR2B (for NR2B) antibodies. Images show magnified regions of dendritic segments. Scale bar represents 25 μm. (B) The number of clusters of synapsin I or NR2B and that double-positive for synapsin I/NR2B in a 50-μm dendrite length was counted. Results are expressed as the means±SEM of 5 separate cultures. *Significant difference from the control group ($p<0.05$).

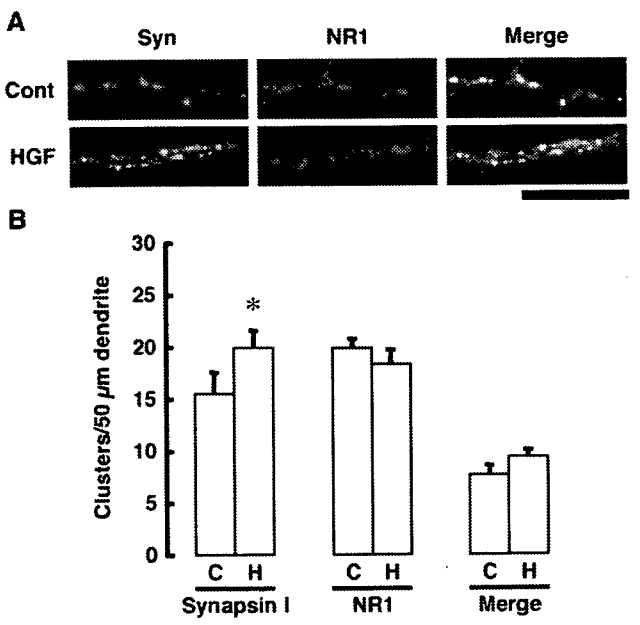

Fig. 3. (A) Hippocampal cells were cultured for 4 days and then treated (H) or not (C) with 30 ng/mL HGF for the following 3 days. The cells were fixed and double-immunostained with anti-synapsin I (for Syn) and anti-NR1 (for NR1) antibodies. Images show magnified regions of dendritic segments. Scale bar represents 25 μm. (B) The number of clusters of synapsin I or NR1 and that double-positive for synapsin I/NR1 in a 50-μm dendrite length was counted. Results are expressed as the means±SEM of 5 separate cultures. *Significant difference from the control group ($p<0.05$).

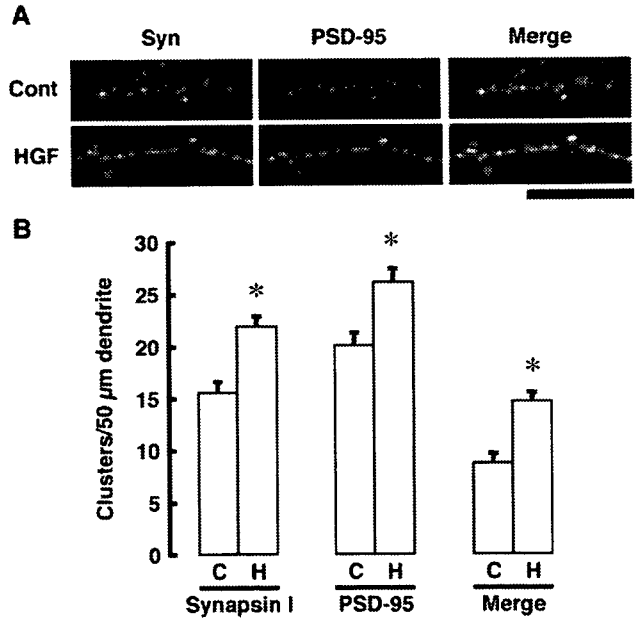

Fig. 5. (A) Hippocampal cells were cultured for 4 days and then treated (H) or not (C) with 30 ng/mL HGF for the following 3 days. The cells were fixed and double-immunostained with anti-synapsin I (for Syn) and anti-PSD-95 (for PSD-95) antibodies. Images show magnified regions of dendritic segments. Scale bar represents 25 μm. (B) The number of clusters of synapsin I or PSD-95 and that double-positive for synapsin I/PSD-95 in a 50-μm dendrite length was counted. Results are expressed as the means±SEM of 5 separate cultures. *Significant difference from the control group ($p<0.05$).

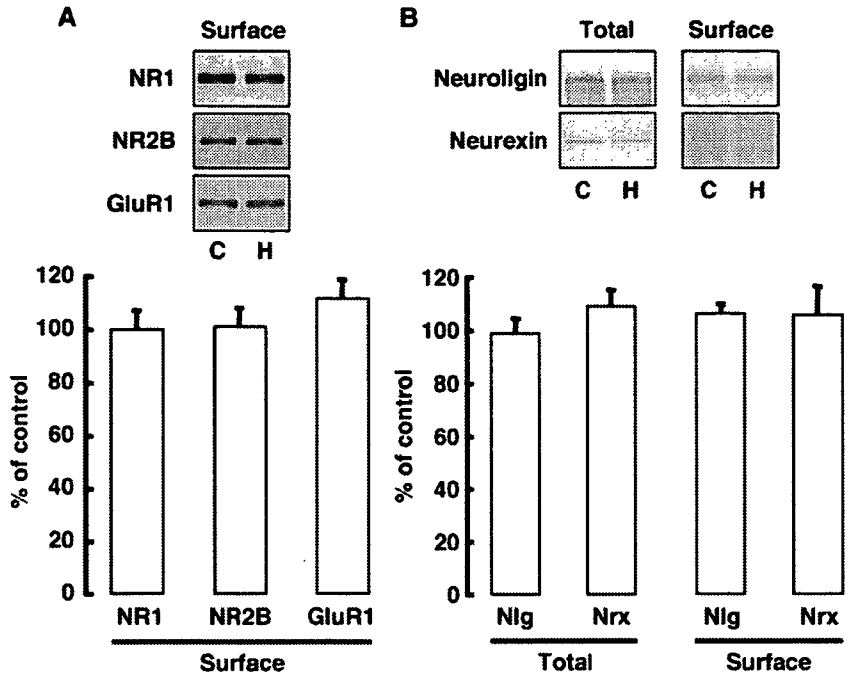

Fig. 6. Four-day hippocampal cultures were incubated in the presence (H) or absence (C) of 30 ng/mL HGF for 3 days. Cell-surface proteins were then labeled with membrane impermeable sulfo-NHS-SS-biotin. Biotinylated proteins were precipitated with avidin beads and analyzed by immunoblotting with anti-NR1, anti-NR2B, and anti-GluR1 antibodies (A) or with anti-neuroligin and anti-neurexin antibodies (B). Total proteins were analyzed by immunoblotting with anti-neuroligin and anti-neurexin antibodies (B). Bands corresponding to NR1, NR2B, and GluR1 (A) or neuroligin and neurexin (B) on immunoblots were scanned. Results are expressed as the average percentages of the control ± SEM of 4 separate cultures.

NMDA receptor subunits NR1 and NR2B (Fig. 6A). The surface expression of AMPA receptor subunit GluR1 was not affected by treatment with HGF (Fig. 6A). At 7 DIV, we further examined the effects of HGF on the expression of neuroligin, which is a binding partner of PSD-95 and connects the PSD to the presynaptic release machinery, and on that of neurexin, which is a presynaptic binding partner of neuroligin. There were no changes in total amounts of neuroligin and neurexin irrespective of HGF treatment (Fig. 6B). The surface expression of these proteins was also unaffected regardless of treatment or not with HGF (Fig. 6B).

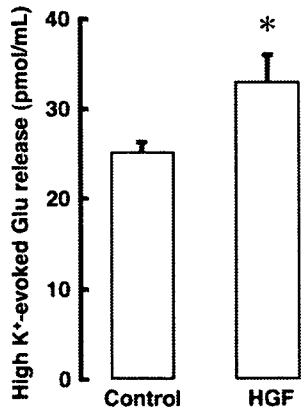

Fig. 7. Hippocampal cells were cultured in the presence (H) or absence (C) of 30 ng/mL HGF for 3 days and then stimulated by high K^+ (60 mM)-evoked depolarization. The amount of released glutamate was quantified by HPLC. Values represent the means ± SEM of 6 separate cultures. *Significant difference from the control group ($p<0.05$).

Although the total amount of synapsin I was not altered irrespective of the HGF treatment, the number of presynaptic clusters of synapsin I was increased. These findings raise the possibility that HGF would affect synaptic transmission. Next, to examine the effect of HGF on depolarization-evoked release of glutamate, we determined the amount of glutamate released into the medium following high-K^+ (60 mM) stimulation at 7 DIV. HGF treatment increased the amount of depolarization-evoked glutamate release relative to the amount released under normal conditions ($F=0.144$, $p=0.045$, Fig. 7).

Discussion

In the present study, we examined the effect of HGF on synapse formation in young hippocampal neurons by focussing excitatory synapses containing the NMDA receptor and PSD-95, which is a receptor-anchoring protein. First, the HGF receptor c-Met protein in cultured hippocampal neurons was detected at 2 DIV and was clearly identified from 4 DIV. Therefore, the treatment with HGF was started at 4 days, and the effect of HGF on synapse formation was examined 3 days later. We found that tyrosine phosphorylation of c-Met was induced by application of HGF, indicating that c-Met protein in cultured hippocampal neurons at 4 DIV could reveal the functional significance of HGF. The findings are consistent with the observations that the c-Met is expressed in developing hippocampus and plays a pivotal role for the maturation of neurons in the hippocampus (Achim et al., 1997; Honda et al., 1995; Jung et al., 1994; Korhonen et al., 2000; Thewke and Seeds, 1999).

Earlier it was demonstrated that brain-derived neurotrophic factor (BDNF) increased the expression level of presynaptic vesicle-associated proteins and promoted GABAergic maturation (Yamada et al., 2002). Other neurotrophic factors may also play a pivotal role in synapse formation during development. However, the effects of HGF on synaptogenesis in young neurons were still not fully understood. We demonstrated that treatment with HGF increased the number of clusters of the presynaptic marker protein synapsin I without causing a change in the total amount of this protein. In contrast, HGF had no effect on the protein expression levels of NMDA receptor subunits NR1 and NR2B or PSD-95. We demonstrated that the number of double-positive immunofluorescent puncta containing synapsin and NR1 or NR2B was not altered by HGF treatment. Furthermore, we demonstrated that the surface expression of NMDA receptor subunits was unaffected irrespective of HGF treatment. These results suggest that HGF had no effect on the number of synapses containing the NMDA receptor in young hippocampal neurons. Interestingly, we found that treatment with HGF increased the number of double-positive immunofluorescent puncta containing synapsin and PSD-95. The finding that the total amount of PSD-95 after the application of HGF was not altered suggests that PSD-95 was translocated to synaptic sites by HGF treatment. The binding of PSD-95 to NR2 subunits has been implicated in not only the localization and anchoring of receptors but also the regulation of ion channel function, synaptic activity, and intracellular signaling (Kim and Sheng, 2004; Migaud et al., 1998; Sattler et al., 1999; Yamada et al., 1999). Therefore, HGF-mediated recruitment of PSD-95 may be involved in structural and functional maturation of synapses containing the NMDA receptor during development.

As it is known that PSD-95 enhances neuroligin-1 clustering and maturation of excitatory synapses at the expense of inhibitory contacts (Prange et al., 2004), we next examined the cell-surface expression of neuroligin and that of neurexin, which is a presynaptic protein that interacts trans-synaptically with postsynaptic neuroligin. We demonstrated that HGF did not alter the surface expression of either molecule. Postsynaptic differentiation is likely to occur prior to formation of a functional active zone at the presynapse in young hippocampal neurons (Gerrow et al., 2006). Furthermore, overexpression of postsynaptic PSD-95 in hippocampal neurons causes maturation of glutamatergic synapses (El-Husseini et al., 2000). Therefore, HGF might promote the distribution of PSD-95 to the postsynaptic membrane for neuronal development, although further studies will be required to determine whether HGF is involved in the development of excitatory synapses. HGF enhances endothelial junctional integrity by increasing the availability of β-catenin (Liu et al., 2002). Interestingly, a synaptic scaffolding molecule is localized at synapses by the action of β-catenin and recruits neuroligin and PSD-95 (Iida et al., 2004).

In addition, a postsynaptic complex of scaffolding protein PSD-95 and neuroligin is likely to modulate the presynaptic release probability of transmitter vesicles (Futai et al., 2007). In the present study, HGF increased the number of clusters of the presynaptic marker synapsin I. Therefore, HGF may promote functional synaptogenesis by recruiting PSD-95 to the postsynaptic membrane, although the number of double-positive immunofluorescent puncta containing synapsin I and NMDA receptor subunit and the expression of surface neuroligin and neurexin were not affected. We demonstrated that depolarization-evoked release of glutamate was enhanced by HGF treatment. Interestingly, the glutamate concentration at the synaptic cleft is likely to be higher when PSD-95 is postsynaptically over-expressed (Futai et al., 2007). The reason for such a higher glutamate concentration is suggested to be the release of more vesicles at synapses; although other possibilities, such as a decrease in the exclusion of released glutamate from the extracellular spaces, cannot be ruled out. Under pathophysiological conditions, such as cerebral ischemia, excessive glutamate release was occurred and induced neuronal injuries. In this sense, HGF exerts protective effects against excitotoxic injuries *in vitro* and *in vivo*. In contrast, glutamate plays an important role in neuronal development (McDonald and Johnston, 1990). Therefore, depolarization-evoked glutamate release promoted by HGF treatment in young hippocampal neurons may be involved in the regulation of neuronal development, but not in the process of excitotoxicity.

Pre- and postsynaptic functions mediated by PSD-95 and related proteins may play a key role in neural development and synaptic plasticity. In this sense, the expression of PSD-95 and neuroligin is increased during the development of the hippocampus (Petralia et al., 2005; Song et al., 1999). Furthermore, PSD-95 is acutely translocated to the postsynaptic contact in response to neuronal activity in the visual cortex (Song et al., 1999).

Earlier it was shown that HGF enhanced synaptic long-term potentiation in the hippocampal CA1 region and also augmented NMDA receptor-mediated currents (Akimoto et al., 2004). Therefore, HGF may modulate not only the release of neurotransmitters but also postsynaptic functions via activation of certain enzymes during the development in young hippocampal neurons.

It was suggested that, in addition to PSD-95, a preformed complex containing guanylate kinase-associated protein (GKAP), SH3, and an ankyrin repeat-containing protein (Shank) might recruit a number of proteins required for maturation of excitatory synapse (Gerrow et al., 2006). Therefore, we cannot rule out the possibility that postsynaptic proteins other than PSD-95 were involved in the synaptogenesis induced by HGF treatment.

Although the mechanisms for synaptic recruitment of PSD-95 after the treatment with HGF are still unknown, the results in the present study suggest that HGF initially regulates the localization of PSD-95, subsequently promotes depolarization-evoked excitatory neurotransmission during development. Because PSD-95 appears to be important in controlling synaptic plasticity and learning (Migaud et al., 1998), HGF may modulate the ability for synaptic maturation and function.

Acknowledgments

This work was supported by the Promotion and Mutual Aid Corporation for Private Schools of Japan.

References

Achim, C.L., Katyal, S., Wiley, C.A., Shiratori, M., Wang, G., Oshika, E., Petersen, B.E., Li, J.M., Michalopoulos, G.K., 1997. Expression of HGF and cMet in the developing and adult brain. Brain Res. Dev. Brain Res. 102, 299–303.

Akimoto, M., Baba, A., Ikeda-Matsuo, Y., Yamada, M.K., Itamura, R., Nishiyama, N., Ikegaya, Y., Matsuki, N., 2004. Hepatocyte growth factor as an enhancer of NMDA currents and synaptic plasticity in the hippocampus. Neuroscience 128, 155–162.

Balkovetz, D.F., Lipschutz, J.H., 1999. Hepatocyte growth factor and the kidney: it is not just for the liver. Int. Rev. Cyt. 186, 225–260.

Das, S., Sasaki, Y.F., Rothe, T., Premkumar, L.S., Takasu, M., Crandall, J.E., Dikkes, P., Conner, D.A., Rayudu, P.V., Cheung, W., Chen, H.S., Lipton, S.A., Nakanishi, N., 1998. Increased NMDA current and spine density in mice lacking the NMDA receptor subunit NR3A. Nature 393, 377–381.

Date, I., Takagi, N., Takagi, K., Kago, T., Matsumoto, K., Nakamura, T., Takeo, S., 2004. Hepatocyte growth factor improved learning and memory dysfunction of microsphere-embolized rats. J. Neurosci. Res. 78, 442–453.

Dean, C., Dresbach, T., 2006. Neuroligins and neurexins: linking cell adhesion, synapse formation and cognitive function. Trends Neurosci. 29, 21–29.

Dingledine, R., Borges, K., Bowie, D., Traynelis, S.F., 1999. The glutamate receptor ion channels. Pharmacol. Rev. 51, 7–61.

El-Husseini, A.E., Schnell, E., Chetkovich, D.M., Nicoll, R.A., Bredt, D.S., 2000. PSD-95 involvement in maturation of excitatory synapses. Science 290, 1364–1368.

Futai, K., Kim, M.J., Hashikawa, T., Scheiffele, P., Sheng, M., Hayashi, Y., 2007. Retrograde modulation of presynaptic release probability through signaling mediated by PSD-95-neuroligin. Nat. Neurosci. 10, 186–195.

Gerrow, K., Romorini, S., Nabi, S.M., Colicos, M.A., Sala, C., El-Husseini, A., 2006. A preformed complex of postsynaptic proteins is involved in excitatory synapse development. Neuron 49, 547–562.

Giacobini, P., Messina, A., Wray, S., Giampietro, C., Crepaldi, T., Carmeliet, P., Fasolo, A., 2007. Hepatocyte growth factor acts as a mitogen and guidance signal for gonadotropin hormone-releasing hormone-1 neuronal migration. J. Neurosci. 27, 431–445.

Hollmann, M., Heinemann, S., 1994. Cloned glutamate receptors. Annu. Rev. Neurosci. 17, 31–108.

Honda, S., Kagoshima, M., Wanaka, A., Tohyama, M., Matsumoto, K., Nakamura, T., 1995. Localization and functional coupling of HGF and c-Met/HGF receptor in rat brain: implication as neurotrophic factor. Brain Res. Mol. Brain Res. 32, 197–210.

Hossain, M.A., Russell, J.C., Gomez, R., Laterra, J., 2002. Neuroprotection by scatter factor/hepatocyte growth factor and FGF-1 in cerebellar granule neurons is phosphatidylinositol 3-kinase/akt-dependent and MAPK/CREB-independent. J. Neurochem. 81, 365–378.

Huettner, J.E., Baughman, R.W., 1986. Primary culture of identified neurons from the visual cortex of postnatal rats. J. Neurosci. 6, 3044–3060.

Iida, J., Hirabayashi, S., Sato, Y., Hata, Y., 2004. Synaptic scaffolding molecule is involved in the synaptic clustering of neuroligin. Mol. Cell. Neurosci. 27, 497–508.

Ishihara, N., Takagi, N., Niimura, M., Takagi, K., Nakano, M., Tanonaka, K., Funakoshi, H., Matsumoto, K., Nakamura, T., Takeo, S., 2005. Inhibition of apoptosis-inducing factor translocation is involved in protective effects of hepatocyte growth factor against excitotoxic cell death in cultured hippocampal neurons. J. Neurochem. 95, 1277–1286.

Ishii, T., Moriyoshi, K., Sugihara, H., Sakurada, K., Kadotani, H., Yokoi, M., Akazawa, C., Shigemoto, R., Mizuno, N., Masu, M., et al., 1993. Molecular characterization of the family of the *N*-methyl-D-aspartate receptor subunits. J. Biol. Chem. 268, 2836–2843.

Jung, W., Castren, E., Odenthal, M., Vande Woude, G.F., Ishii, T., Dienes, H.P., Lindholm, D., Schirmacher, P., 1994. Expression and functional interaction of hepatocyte growth factor-scatter factor and its receptor c-met in mammalian brain. J. Cell Biol. 126, 485–494.

Kennedy, M.B., 1997. The postsynaptic density at glutamatergic synapses. Trends Neurosci. 20, 264–268.

Kim, E., Sheng, M., 2004. PDZ domain proteins of synapses. Nat. Rev., Neurosci. 5, 771–781.

Klauck, T.M., Scott, J.D., 1995. The postsynaptic density: a subcellular anchor for signal transduction enzymes. Cell. Signal. 7, 747–757.

Korhonen, L., Sjoholm, U., Takei, N., Kern, M.A., Schirmacher, P., Castren, E., Lindholm, D., 2000. Expression of c-Met in developing rat hippocampus: evidence for HGF as a neurotrophic factor for calbindin D-expressing neurons. Eur. J. Neurosci. 12, 3453–3461.

Lavezzari, G., McCallum, J., Dewey, C.M., Roche, K.W., 2004. Subunit-specific regulation of NMDA receptor endocytosis. J. Neurosci. 24, 6383–6391.

Liu, F., Schaphorst, K.L., Verin, A.D., Jacobs, K., Birukova, A., Day, R.M., Bogatcheva, N., Bottaro, D.P., Garcia, J.G., 2002. Hepatocyte growth factor enhances endothelial cell barrier function and cortical cytoskeletal rearrangement: potential role of glycogen synthase kinase-3beta. FASEB J. 16, 950–962.

Lin, Y., Skeberdis, V.A., Francesconi, A., Bennett, M.V., Zukin, R.S., 2004. Postsynaptic density protein-95 regulates NMDA channel gating and surface expression. J. Neurosci. 24, 10138–10148.

Machide, M., Kamitori, K., Nakamura, Y., Kohsaka, S., 1998. Selective activation of phospholipase C gamma1 and distinct protein kinase C subspecies in intracellular signaling by hepatocyte growth factor/scatter factor in primary cultured rat neocortical cells. J. Neurochem. 71, 592–602.

Matsumoto, K., Nakamura, T., 1996. Emerging multipotent aspects of hepatocyte growth factor. J. Biochem. (Tokyo) 119, 591–600.

Matsumoto, K., Nakamura, T., 2001. Hepatocyte growth factor: renotropic role and potential therapeutics for renal diseases. Kidney Int. 59, 2023–2038.

McDonald, J.W., Johnston, M.V., 1990. Physiological and pathophysiological roles of excitatory amino acids during central nervous system development. Brain Res. Brain Res. Rev. 15, 41–70.

Migaud, M., Charlesworth, P., Dempster, M., Webster, L.C., Watabe, A.M., Makhinson, M., He, Y., Ramsay, M.F., Morris, R.G., Morrison, J.H., O'Dell, T.J., Grant, S.G., 1998. Enhanced long-term potentiation and impaired learning in mice with mutant postsynaptic density-95 protein. Nature 396, 433–439.

Monyer, H., Sprengel, R., Schoepfer, R., Herb, A., Higuchi, M., Lomeli, H., Burnashev, N., Sakmann, B., Seeburg, P.H., 1992. Heteromeric NMDA receptors: molecular and functional distinction of subtypes. Science 256, 1217–1221.

Morishita, R., Nakamura, S., Hayashi, S., Taniyama, Y., Moriguchi, A., Nagano, T., Taiji, M., Noguchi, H., Takeshita, S., Matsumoto, K., Nakamura, T., Higaki, J., Ogihara, T., 1999. Therapeutic angiogenesis induced by human recombinant hepatocyte growth factor in rabbit hind limb ischemia model as cytokine supplement therapy. Hypertension 33, 1379–1384.

Moriyoshi, K., Masu, M., Ishii, T., Shigemoto, R., Mizuno, N., Nakanishi, S., 1991. Molecular cloning and characterization of the rat NMDA receptor. Nature 354, 31–37.

Nakamura, T., Nawa, K., Ichihara, A., 1984. Partial purification and characterization of hepatocyte growth factor from serum of hepatectomized rats. Biochem. Biophys. Res. Commun. 122, 1450–1459.

Nakamura, T., Nishizawa, T., Hagiya, M., Seki, T., Shimonishi, M., Sugimura, A., Tashiro, K., Shimizu, S., 1989. Molecular cloning and expression of human hepatocyte growth factor. Nature 342, 440–443.

Nakamura, T., Mizuno, S., Matsumoto, K., Sawa, Y., Matsuda, H., Nakamura, T., 2000. Myocardial protection from ischemia/reperfusion injury by endogenous and exogenous HGF. J. Clin. Invest. 106, 1511–1519.

Nakanishi, S., 1992. Molecular diversity of glutamate receptors and implications for brain function. Science 258, 597–603.

Niimura, M., Takagi, N., Takagi, K., Mizutani, R., Ishihara, N., Matsumoto, K., Funakoshi, H., Nakamura, T., Takeo, S., 2006. Prevention of apoptosis-inducing factor translocation is a possible mechanism for protective effects of hepatocyte growth factor against neuronal cell death in the hippocampus after transient forebrain ischemia. J. Cereb. Blood Flow Metab. 26, 1354–1365.

Nishi, M., Hinds, H., Lu, H.P., Kawata, M., Hayashi, Y., 2001. Motoneuron-specific expression of NR3B, a novel NMDA-type glutamate receptor subunit that works in a dominant-negative manner. J. Neurosci. 21, RC185.

Ohya, W., Funakoshi, H., Kurosawa, T., Nakamura, T., 2007. Hepatocyte growth factor (HGF) promotes oligodendrocyte progenitor cell proliferation and inhibits its differentiation during postnatal development in the rat. Brain Res. 1147, 51–65.

Petralia, R.S., Sans, N., Wang, Y.X., Wenthold, R.J., 2005. Ontogeny of postsynaptic density proteins at glutamatergic synapses. Mol. Cell. Neurosci. 29, 436–452.

Prange, O., Wong, T.P., Gerrow, K., Wang, Y.T., El-Husseini, A., 2004. A balance between excitatory and inhibitory synapses is controlled by PSD-95 and neuroligin. Proc. Natl. Acad. Sci. U. S. A. 101, 13915–13920.

Rao, A., Kim, E., Sheng, M., Craig, A.M., 1998. Heterogeneity in the molecular composition of excitatory postsynaptic sites during development of hippocampal neurons in culture. J. Neurosci. 18, 1217–1229.

Roche, K.W., Standley, S., McCallum, J., Dune Ly, C., Ehlers, M.D., Wenthold, R.J., 2001. Molecular determinants of NMDA receptor internalization. Nat. Neurosci. 4, 794–802.

Sattler, R., Xiong, Z., Lu, W.Y., Hafner, M., MacDonald, J.F., Tymianski, M., 1999. Specific coupling of NMDA receptor activation to nitric oxide neurotoxicity by PSD-95 protein. Science 284, 1845–1848.

Shen, L., Liang, F., Walensky, L.D., Huganir, R.L., 2000. Regulation of AMPA receptor GluR1 subunit surface expression by a 4.1N-linked actin cytoskeletal association. J. Neurosci. 20, 7932–7940.

Song, J.Y., Ichtchenko, K., Sudhof, T.C., Brose, N., 1999. Neuroligin 1 is a postsynaptic cell-adhesion molecule of excitatory synapses. Proc. Natl. Acad. Sci. U. S. A. 96, 1100–1105.

Sun, W., Funakoshi, H., Nakamura, T., 2002a. Localization and functional role of hepatocyte growth factor (HGF) and its receptor c-met in the rat developing cerebral cortex. Brain Res. Mol. Brain Res. 103, 36–48.

Sun, W., Funakoshi, H., Nakamura, T., 2002b. Overexpression of HGF retards disease progression and prolongs life span in a transgenic mouse model of ALS. J. Neurosci. 22, 6537–6548.

Thewke, D.P., Seeds, N.W., 1999. The expression of mRNAs for hepatocyte growth factor/scatter factor, its receptor c-met, and one of its activators tissue-type plasminogen activator show a systematic relationship in the developing and adult cerebral cortex and hippocampus. Brain Res. 821, 356–367.

Ueda, H., Nakamura, T., Matsumoto, K., Sawa, Y., Matsuda, H., Nakamura, T., 2001. A potential cardioprotective role of hepatocyte growth factor in myocardial infarction in rats. Cardiovasc. Res. 51, 41–50.

Van Belle, E., Witzenbichler, B., Chen, D., Silver, M., Chang, L., Schwall, R., Isner, J.M., 1998. Potentiated angiogenic effect of scatter factor/hepatocyte growth factor via induction of vascular endothelial growth factor: the case for paracrine amplification of angiogenesis. Circulation 97, 381–390.

Yamada, Y., Chochi, Y., Takamiya, K., Sobue, K., Inui, M., 1999. Modulation of the channel activity of the epsilon2/zeta1-subtype *N*-methyl D-aspartate receptor by PSD-95. J. Biol. Chem. 274, 6647–6652.

Yamada, M.K., Nakanishi, K., Ohba, S., Nakamura, T., Ikegaya, Y., Nishiyama, N., Matsuki, N., 2002. Brain-derived neurotrophic factor promotes the maturation of GABAergic mechanisms in cultured hippocampal neurons. J. Neurosci. 22, 7580–7585.

Zarnegar, R., Michalopoulos, G.K., 1995. The many faces of hepatocyte growth factor: from hepatopoiesis to hematopoiesis. J. Cell Biol. 129, 1177–1180.

Ziff, E.B., 1997. Enlightening the postsynaptic density. Neuron 19, 1163–1174.

Available online at www.sciencedirect.com
ScienceDirect
Neuroscience Research 59 (2007) 446–456
Neuroscience Research
www.elsevier.com/locate/neures

Hepatocyte growth factor (HGF) attenuates gliosis and motoneuronal degeneration in the brainstem motor nuclei of a transgenic mouse model of ALS

Keiichi Kadoyama, Hiroshi Funakoshi, Wakana Ohya, Toshikazu Nakamura *

Division of Molecular Regenerative Medicine, Department of Biochemistry and Molecular Biology, Osaka University Graduate School of Medicine, Osaka 565-0871, Japan

Received 20 July 2007; accepted 20 August 2007
Available online 31 August 2007

Abstract

Amyotrophic lateral sclerosis (ALS) is a fatal neurodegenerative disease characterized by progressive loss of brainstem and spinal motoneurons. Although prevention of motoneuronal degeneration has been postulated as the primary target for a cure, accumulating evidence suggests that microglial accumulation contributes to disease progression. This study was designed to assess the ability of HGF to modulate microglial accumulation and motoneuronal degeneration in brainstem motor nuclei, using double transgenic mice overexpressing mutated $SOD1^{G93A}$ and HGF (G93A/HGF). Histological and immunohistochemical analyses of the tissues of G93A/HGF mice revealed a marked decrease in the number of microglia and reactive astrocytes and an attenuation of the loss of motoneurons in facial and hypoglossal nuclei compared with G93A mice. HGF overexpression attenuated monocyte chemoattractant protein-1 (MCP-1) induction, predominantly in astrocytes; suppressed activation of caspase-1, -3 and -9; and, increased X chromosome-linked inhibition of apoptosis protein (XIAP) in the motoneurons of G93A mice. The implication is that HGF reduces microglial accumulation by suppressing MCP-1 induction and prevents motoneuronal death through inhibition of pro-apoptotic protein activation. These findings suggest that, in addition to direct neurotrophic activity on motoneurons, HGF-suppression of gliosis may retard disease progression, making HGF a potential therapeutic agent for the treatment of ALS patients.

Keywords: Caspases; X chromosome-linked inhibitor of apoptosis protein (XIAP); Microglia; Monocyte chemoattractant protein-1 (MCP-1); c-Met

1. Introduction

Amyotrophic lateral sclerosis (ALS) is a fatal neurodegenerative disease characterized by progressive degeneration of motoneurons and their axons in the brainstem and spinal cord, leading to spasticity, hyperreflexia, generalized weakness of the limbs, muscle atrophy, and paralysis (Cleveland and Rothstein, 2001). Most cases (90%) are classified as sporadic ALS (SALS), as they are not associated with a documented family history. The remaining 10% are inherited and referred to as familial ALS (FALS). Gene mutations in copper/zinc superoxide dismutase 1 (SOD1) are responsible for 15–20% of FALS. In addition, mutations in the ALS2/alsin, senataxin (SETX), synaptobrevin/vesicle-associated membrane protein-associated protein B (VAPB) and dynactin genes recently have been associated with ALS (Pasinelli and Brown, 2006). Regardless of the type of gene mutations or whether the disease is familial or sporadic, motoneuronal degeneration is thought to constitute a common and primary event in ALS (Cleveland and Rothstein, 2001). Therefore, most efforts have been directed toward finding molecules that act directly on motoneurons in an attempt to reduce their degeneration, regardless of the effects of gliosis on surrounding motoneurons. However, treatment with minocycline, an antibiotic that inhibits microglial activation (Yrjanheikki et al., 1999; Van Den Bosch et al., 2002; Zhu et al., 2002), was found to slow disease progression in a transgenic mouse model of ALS that overexpresses mutated human $SOD1^{G93A}$ (G93A) (Kriz et al., 2002). Boillee et al. (2006) recently used the Cre-lox system to show that diminishing expression of mutated $SOD1^{G37R}$ in the microglia of a transgenic mouse model of ALS prolongs disease duration and survival. These lines of evidence demonstrate that

* Corresponding author. Tel.: +81 6 6879 3783; fax: +81 6 6879 3789.
E-mail address: nakamura@onbich.med.osaka-u.ac.jp (T. Nakamura).

0168-0102/$ – see front matter © 2007 Elsevier Ireland Ltd and the Japan Neuroscience Society. All rights reserved.
doi:10.1016/j.neures.2007.08.017

microglia might contribute to disease progression that is caused by mutant SOD1 toxicity in a transgenic mouse model of ALS and raises the possibility that reducing the number of activated microglia could be incorporated as another strategy for ALS therapy.

Hepatocyte growth factor (HGF) was initially identified and molecularly cloned as a potent mitogen for mature hepatocytes (Nakamura et al., 1984, 1989). Subsequent studies revealed that HGF exerts multiple biological effects, including mitogenic, motogenic, morphogenic, and anti-apoptotic activities in a wide variety of cells, including neurons, by binding to the c-Met receptor tyrosine kinase (c-Met) (Funakoshi and Nakamura, 2003). HGF is one of the most potent *in vitro* and *in vivo* survival-promoting factors for neurons. For example, neurotrophic effects of HGF have been demonstrated in cultured hippocampal neurons (Honda et al., 1995) and in cultured embryonic spinal motoneurons (Ebens et al., 1996; Yamamoto et al., 1997; Novak et al., 2000), and its anti-apoptotic activity in motoneurons is comparable to that of glial cell line-derived neurotrophic factor (GDNF) (Ebens et al., 1996). Indeed, reflecting the *in vitro* neurotrophic activity of HGF on motoneurons and the expression of c-Met in motoneurons of G93A mice, the transgenic overexpression of rat HGF in the nervous system attenuates spinal motoneuronal death and axonal degeneration, delays onset of the disease and prolongs the lifespan of G93A mice (Sun et al., 2002). However, many studies have suggested that some neurotrophic factors show survival-promoting effects only on certain subtypes of motoneurons in the spinal cord and brainstem (Sakamoto et al., 2003; Guillot et al., 2004). Therefore, the effects of HGF on the degeneration of ALS brainstem motoneurons in G93A mice remain unclear. Furthermore, the role of HGF on microglial accumulation, another research target in the search for an ALS cure, is poorly understood. In the present study, the effects of HGF on microglial accumulation and motoneuronal degeneration in brainstem (facial and hypoglossal) motor nuclei of G93A mice were examined using double transgenic mice overexpressing mutated human $SOD1^{G93A}$ and HGF. The molecular mechanisms by which HGF functions in suppressing microglial accumulation and attenuating motoneuronal degeneration in G93A mice were also examined.

2. Materials and methods

2.1. Animals

Neuron-specific enolase promoter-driven HGF transgenic (HGF-Tg) mice were generated as previously described (Sun et al., 2002). Transgenic mice overexpressing mutated (glycine to alanine in position 93) human SOD1 (G93A) [B6SJL-TgN (SOD1-G93A)^{dl}Gur1] (Gurney et al., 1994) were purchased from the Jackson Laboratory (Bar Harbor, ME). This mouse strain has a low copy number of $SOD1^{G93A}$ and shows a delayed onset of ALS, slower disease progression, and a longer lifespan compared with mice carrying a high copy number of the transgene (G1H). This strain resembles the slow progressing phenotype of patients with ALS and is useful for the accurate evaluation of the molecular mechanisms involved in the action of HGF during disease progression. HGF-Tg mice were crossed with G93A transgenic mice to generate G93A/HGF-double transgenic animals. The HGF and G93A transgenic heterozygous mice were maintained by mating transgenic males with C57/BL6 females. Mouse genotypes were determined by polymerase chain reaction (PCR) and Southern blot analysis as previously reported (Gurney et al., 1994; Sun et al., 2002). Non-transgenic littermates served as controls. Experimental protocols were approved by the Animal Experimentation Ethics Committee of Osaka University Graduate School of Medicine. All efforts were made to minimize animal discomfort and the number of animals used.

2.2. Tissue preparation

Wild-type (WT), HGF-Tg, G93A, and G93A/HGF mice at 6 and 8 months of age were sacrificed with an overdose injection of pentobarbital sodium salt. Tissues were fixed by treating them in increasing concentrations of ethanol. After dehydration, the tissues were treated with xylene and embedded in paraffin. Serial tissue sections were cut on a microtome to a thickness of 7 μm, deparaffinized, and used for either Nissl staining or for immunohistochemistry.

2.3. Motoneuron survival

The neuroprotective effect of HGF on facial and hypoglossal motoneurons was evaluated by counting the number of motoneurons (i.e., motoneuronal survival). The number of motoneurons in the facial and hypoglossal nuclei of WT, HGF-Tg, G93A, and G93A/HGF mice were counted in every fifth section of 16 Nissl-stained 7-μm-thick paraffin sections ($n = 4$). Densely stained motoneurons with a clear nucleolus and in a defined area of facial and hypoglossal nuclei were counted using Win ROOF analysis software (Mitani Corp., Fukui, Japan) as previously described (Sun et al., 2002).

2.4. HGF ELISA

HGF protein levels in the brainstem of WT and HGF-Tg mice were measured by ELISA using an anti-rat HGF polyclonal antibody (Tokushu Meneki, Tokyo, Japan) as previously described (Sun et al., 2002).

2.5. Immunohistochemistry

The sections were stained with the following antibodies: (i) c-Met polyclonal antibody (1:50; Santa Cruz Biotech, Santa Cruz, CA); (ii) tubulinßIII monoclonal antibody (1:500; Berkeley Antibody Co. Inc., Richmond, CA); (iii) caspase-1 (p10) polyclonal antibody (1:100; Santa Cruz Biotech); (iv) active caspase-3 polyclonal antibody (1:200; Promega, Madison, WI) (v) cleaved caspase-9 polyclonal antibody (1:50; Cell Signaling Technology, Beverly, MA); (vi) X chromosome-linked inhibitor of apoptosis protein (XIAP) monoclonal antibody (1:50; BD Pharmingen, San Diego, CA); (vii) glial fibrillary acidic protein (GFAP) monoclonal antibody (1:500; Chemicon International, Temecula, CA); (viii) Iba1 polyclonal antibody (1:2000; Wako Pure Chemical, Osaka, Japan); and (ix) monocyte chemoattractant protein (MCP)-1 polyclonal antibody (1:100; Abcam, Cambridge, UK). These antibodies were applied to the sections for 1 h at room temperature (RT) or overnight at 4 °C after blocking with phosphate-buffered saline (PBS) containing 5% goat serum and 0.1% Triton X-100 at RT for 1 h. After washing the sections with PBS, immunoreactivity (IR) was visualized by incubating them for 20 min at RT with secondary antibodies conjugated with Alexa Fluor 488 (green) or Alexa Fluor 546 (red) diluted 1:500 (Invitrogen, Carlsbad, CA). When double-immunostaining for XIAP and tubulinßIII was performed, antibodies against XIAP and tubulinßIII were labeled with Alexa Fluor 546 and 488, respectively, using a Zenon labeling kit according to the manufacturer's instructions (Invitrogen). These fluorescence-immunostained sections were observed under a LSM 5 PASCAL confocal microscope (Carl Zeiss, Germany). The staining specificity of the antibodies was also assessed by the absence with first antibody or by preincubation with an excess amount of immunized peptide. The intensities of immunoreactivity against GFAP, Iba-1, MCP-1, active caspase-1, -3, -9 and XIAP were determined as previously described (Sun et al., 2002).

2.6. Statistical analysis

Results were expressed as the mean ± S.E. Statistically significant differences among the four groups of mice were assessed by ANOVA, followed by

Scheffe's post hoc test. Statistical significance was defined as $P < 0.05$ or $P < 0.01$.

3. Results

3.1. c-Met is expressed in facial and hypoglossal motoneurons in a transgenic mouse model of ALS

The effect of HGF on gliosis and motoneuronal degeneration was investigated using a mouse model of ALS (G93A) in which mutated human $SOD1^{G93A}$ is overexpressed (Gurney et al., 1994). Expression of the c-Met/HGF receptor (c-Met) was examined in the facial and hypoglossal nuclei of wild-type (WT) and G93A mice. Immunofluorescence analysis with antibodies against c-Met and tubulinßIII (a neuronal marker) showed that c-Met immunoreactivity (IR) was detectable in the facial and hypoglossal nuclei, and that it was localized in the large-size neurons of WT and G93A mice at both 6 (data not shown) and 8 months (Fig. 1a) of age. These results demonstrate that c-Met is present in facial and hypoglossal motoneurons of WT and G93A mice at the ages that correspond to the middle and end stages of the disease.

3.2. Introduction of HGF into the brainstem of transgenic mice overexpressing HGF (HGF-Tg)

The role of HGF was examined using transgenic mice overexpressing rat HGF (HGF-Tg) (Sun et al., 2002). In HGF-Tg mice, exogenous rat HGF mRNA is located specifically in the brain and spinal cord, as evidenced by an RNase protection assay (Sun et al., 2002). An HGF ELISA, which specifically recognizes rodent HGF, revealed that the levels of HGF in the brainstem of HGF-Tg mice were 2-fold higher than in WT mice (Fig. 1b) with no effect on serum HGF levels (data not shown), demonstrating the successful introduction of HGF into the brainstem of HGF-Tg mice.

3.3. Neuroprotective effect of HGF on facial and hypoglossal motoneurons in G93A mice

The effect of HGF on facial and hypoglossal nuclei against ALS was evaluated by generating double transgenic mice (G93A × HGF-Tg) that overexpressed a mutated form of human $SOD1^{G93A}$ and rat HGF (G93A/HGF). This mating resulted in the generation of four groups of mice: (1) WT, (2) HGF-Tg, (3) G93A and (4) G93A/HGF. Nissl staining showed that the facial motoneurons of G93A mice at 8 months of age were atrophic and were present in lower numbers compared with WT and HGF-Tg mice (Fig. 2a), i.e., 55% of WT (Fig. 2b). In contrast, the facial motoneurons of G93A/HGF mice exhibited a healthier morphology (i.e., less atrophic) than those of G93A mice (Fig. 2a). The mean number of facial motoneurons in G93A/HGF mice was significantly larger than that of the G93A mice, and was almost the same as that of WT mice (Fig. 2b).

The hypoglossal motoneurons of G93A mice also were atrophic, and reduced in number compared with WT and HGF-Tg mice (Fig. 2c), with a decrease in mean number to 57% of WT mice (Fig. 2d). Similar to the facial motoneurons of G93A/HGF mice, the hypoglossal motoneurons of G93A/HGF mice also exhibited a healthier morphology than did those of G93A mice (Fig. 2c). The mean number of hypoglossal motoneurons of G93A/HGF mice was significantly larger than that found in G93A mice (Fig. 2d). These results demonstrate that HGF exerts a neuroprotective effect on brainstem motoneurons against ALS-associated neurotoxicity.

3.4. HGF suppresses gliosis in facial and hypoglossal nuclei of G93A mice

The effect of HGF on gliosis in facial and hypoglossal nuclei of G93A mice was examined using antibodies against Iba1

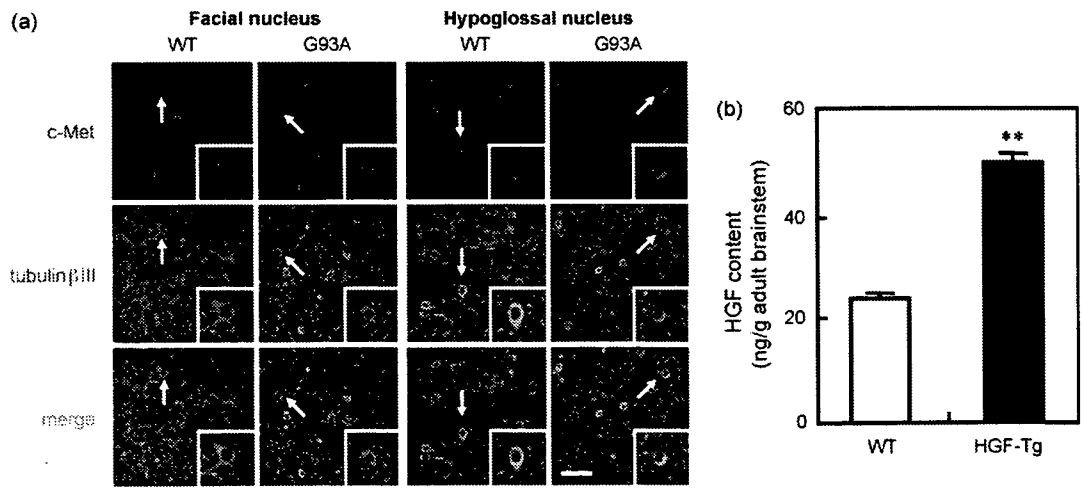

Fig. 1. Expression of c-Met and HGF in the brainstem. (a) Double-immunofluorescence analysis for c-Met (red) and tubulinßIII (green; a marker for neurons) in the facial and hypoglossal nuclei of WT and G93A mice at 8 months of age. A high-magnification view of the area indicated by the arrow is also boxed in each photo. c-Met immunoreactivity was detectable in large-sized neurons of the facial and hypoglossal nuclei. Scale bar = 50 μm. (b) Protein levels of HGF in the brainstems of 6-month-old wild-type (WT) and HGF transgenic (HGF-Tg) mice were analyzed by ELISA ($n = 6$ in each group). Data represent the mean ± S.E. $^{**}P < 0.01$ compared with WT mice.

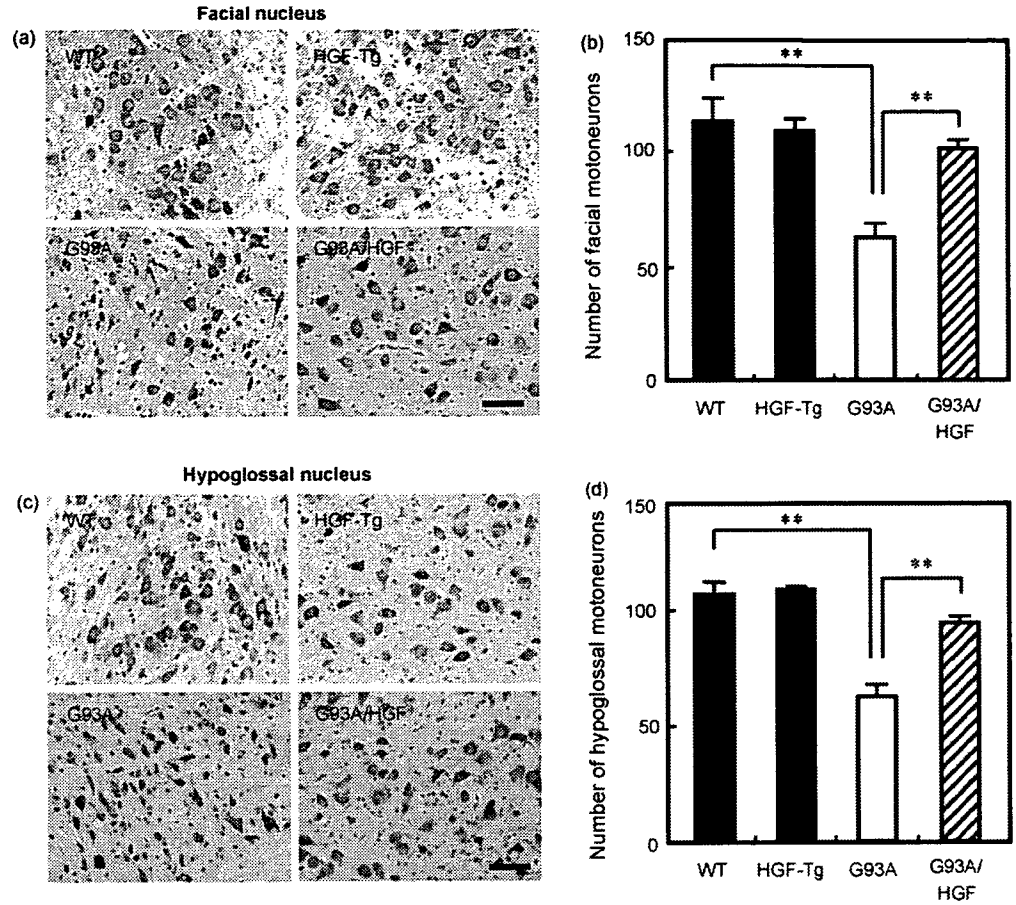

Fig. 2. Neuroprotective effect of HGF on facial (a and b) and hypoglossal (c and d) motoneurons in G93A mice. (a and c) Photomicrographs of representative Nissl-stained sections of the facial (a) and hypoglossal (c) nuclei of WT, HGF-Tg, G93A, and G93A/HGF mice at 8 months of age are shown. Scale bars = 50 μm. (b and d) Quantification of the mean numbers of surviving Nissl-stained neuronal cells with a clear nucleolus in the facial (b) and hypoglossal (d) nuclei of 8-month-old mice of each group. Motoneuron survival is expressed as the neuronal cell count on every fifth section of 16 sections. Data represent the mean ± S.E. (n = 4 for each group). $^{**}P < 0.01$ compared with WT and G93A/HGF mice.

(a microglia marker; Imai et al., 1996) and GFAP (an astrocyte marker). As shown in Fig. 3a, microglia densely accumulated in the facial nuclei of G93A mice at 8 months of age, while the number of microglia was lower in the facial nuclei of WT and HGF-Tg mice. The mean intensity of Iba1-IR in the facial nuclei of G93A mice increased 3.7-fold over the WT signal. In contrast, the mean intensity of Iba1-IR in the facial nuclei of G93A/HGF mice decreased to 59% of that found in G93A mice. Similar results were obtained for the hypoglossal nuclei (Fig. 3a).

Immunofluorescence analyses showed that a large number of hypertrophic astrocytes (i.e., exhibiting astrocytosis) were evident in the facial and hypoglossal nuclei of the G93A mice, while the number of astrocytes was low in the nuclei of both WT and HGF-Tg mice. Consistent with the reduction of Iba1-IR and GFAP-IR, the numbers of Iba1-positive and GFAP-positive cells were lower in G93A/HGF mice compared with G93A mice (data not shown). These results demonstrate that HGF is capable of suppressing both microgliosis (accumulation of activated microglia) and astrocytosis in the facial and hypoglossal nuclei of G93A mice.

3.5. HGF suppresses active caspase-1 and monocyte chemoattractant protein (MCP)-1 in facial and hypoglossal nuclei of G93A mice

The mechanisms by which HGF suppresses gliosis in the facial and hypoglossal nuclei of G93A mice were examined. The mRNA expression of monocyte chemoattractant protein (MCP)-1 is critical for recruitment of inflammatory cells of the monocytic lineage after inflammation or injury to the central nervous system (Berman et al., 1996). Compared with non-neurological disease controls, MCP-1 is markedly increased in the spinal cords of ALS patients and in transgenic mice overexpressing $SOD1^{G37R}$ (G37R mice, a model of ALS) (Henkel et al., 2004, 2006; Baron et al., 2005). Intrathecal treatment with cyclosporin, which is thought to reduce MCP-1 levels, prolongs survival of late stage G93A mice (Keep et al., 2001). Therefore, HGF modulation of MCP-1 levels in the facial and hypoglossal nuclei of 8-month-old G93A mice was examined using immunohistochemistry. MCP-1-IR primarily localized to astrocyte-like cells in the facial nuclei of G93A mice. Double-fluorescence immunostaining revealed that MCP-1-IR with strong immunoreactivity co-localized well

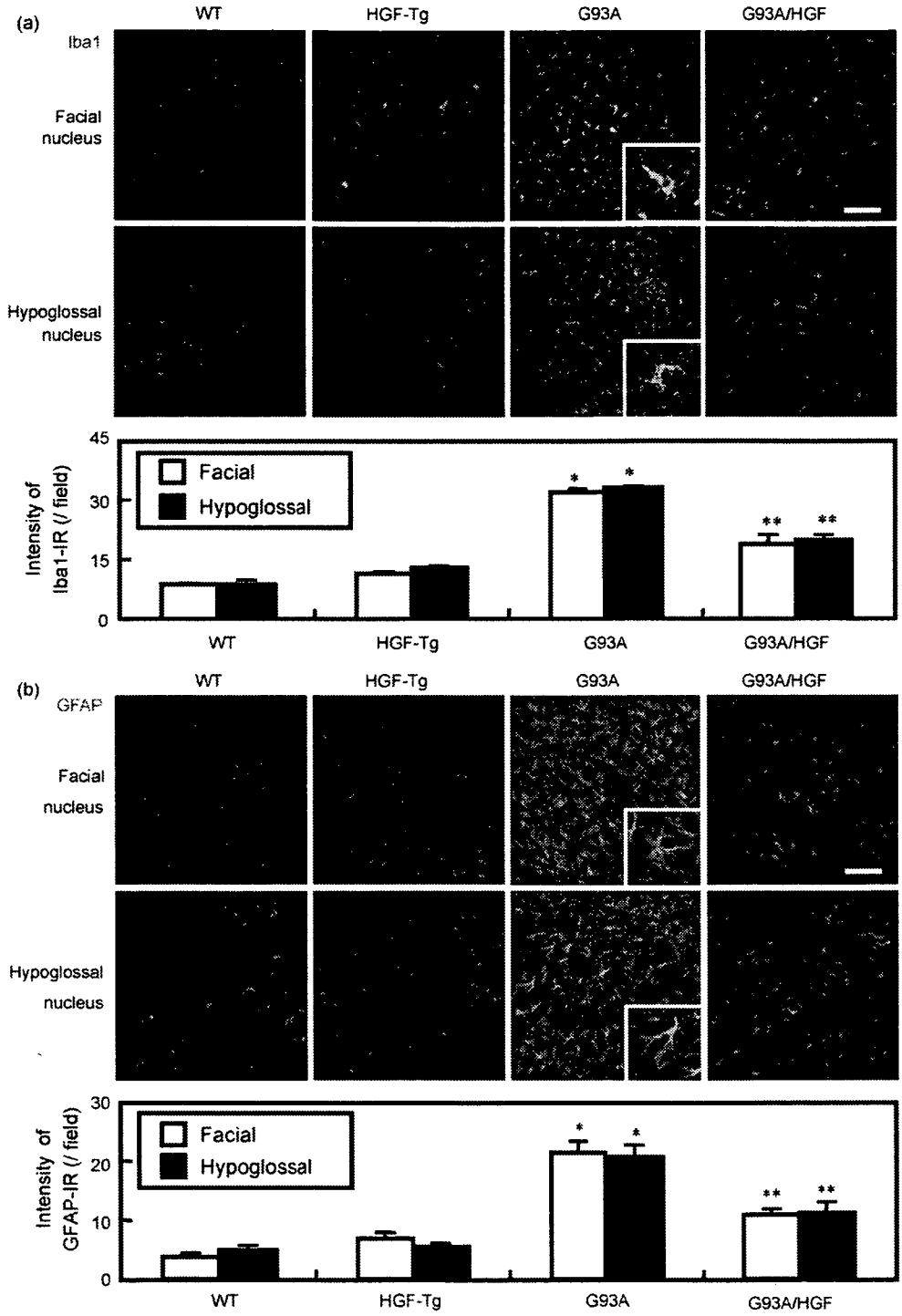

Fig. 3. Suppression of gliosis in the facial and hypoglossal nuclei of G93A/HGF mice. (a) Suppression of microglial accumulation in G93A/HGF mice. Immunofluorescence analysis for Iba1 (a marker for microglia) in the facial and hypoglossal nuclei of WT, HGF-Tg, G93A and G93A/HGF mice at 8 months of age. Scale bar = 100 μm. The intensity of Iba1-IR is shown in the facial (open column) and hypoglossal (closed column) nuclei. Data represent the mean ± S.E. ($n = 4$ for each group). *$P < 0.05$ vs. WT mice and **$P < 0.05$ vs. G93A mice. (b) Suppression of astrocytosis in G93A/HGF mice. Immunofluorescence analysis for GFAP (a marker for astrocyte) in the facial and hypoglossal nuclei of WT, HGF-Tg, G93A and G93A/HGF mice at 8 months of age. Scale bar = 100 μm. The intensity of GFAP-IR is shown in the facial (open column) and hypoglossal (closed column) nuclei. Data represent the mean ± S.E. ($n = 4$ for each group). *$P < 0.05$ vs. WT mice and **$P < 0.05$ vs. G93A mice.

with GFAP, indicating that MCP-1-IR is predominantly induced in reactive astrocytes (Fig. 4a, upper left panel). While double-fluorescence immunostaining of MCP-1 and tubulinßIII showed that weakly immunostained MCP-1-IR cells in G93A mice were motoneurons, the signal was below the detection limit in the facial nuclei of WT mice (Fig. 4a, upper middle panel). In contrast with G93A mice, G93A/HGF mice showed much lower levels of MCP-1-IR in the facial nuclei